



**HAL**  
open science

## Direct observations of the atmospheric processing of Asian mineral dust

R. C. Sullivan, S. A. Guazzotti, D. A. Sodeman, K. A. Prather

► **To cite this version:**

R. C. Sullivan, S. A. Guazzotti, D. A. Sodeman, K. A. Prather. Direct observations of the atmospheric processing of Asian mineral dust. *Atmospheric Chemistry and Physics Discussions*, 2006, 6 (3), pp.4109-4170. hal-00301317

**HAL Id: hal-00301317**

**<https://hal.science/hal-00301317>**

Submitted on 18 Jun 2008

**HAL** is a multi-disciplinary open access archive for the deposit and dissemination of scientific research documents, whether they are published or not. The documents may come from teaching and research institutions in France or abroad, or from public or private research centers.

L'archive ouverte pluridisciplinaire **HAL**, est destinée au dépôt et à la diffusion de documents scientifiques de niveau recherche, publiés ou non, émanant des établissements d'enseignement et de recherche français ou étrangers, des laboratoires publics ou privés.

Processing of Asian  
dust

R. C. Sullivan et al.

# Direct observations of the atmospheric processing of Asian mineral dust

R. C. Sullivan<sup>1</sup>, S. A. Guazzotti<sup>1</sup>, D. A. Sodeman<sup>1,\*</sup>, and K. A. Prather<sup>1,2</sup>

<sup>1</sup>Department of Chemistry & Biochemistry, University of California, San Diego, La Jolla, CA, 92093-0314, USA

<sup>2</sup>Scripps Institution of Oceanography, University of California, San Diego, La Jolla, CA, 92093, USA

\*now at: Desert Research Institute, Reno, NV, USA, 89512

Received: 6 March 2006 – Accepted: 15 March 2006 – Published: 23 May 2006

Correspondence to: K. A. Prather (kprather@ucsd.edu)

Title Page

Abstract

Introduction

Conclusions

References

Tables

Figures

◀

▶

◀

▶

Back

Close

Full Screen / Esc

Printer-friendly Version

Interactive Discussion

EGU

## Abstract

The accumulation of secondary acid products and ammonium on individual mineral dust particles during ACE-Asia has been measured in real-time using ATOFMS. Changes in the amounts of sulphate, nitrate, and chloride mixed with dust particles corresponded to different air mass source regions. During volcanically influenced periods, dust mixed with sulphate dominated. This rapidly switched to dust predominantly mixed with chloride when the first Asian dust front reached the R/V Ronald Brown. We hypothesise that the high degree of mixing of dust with chloride was caused by the prior reaction of  $\text{NO}_y(\text{g})$  and volcanic  $\text{SO}_2(\text{g})$  with sea salt particles, reducing the availability of nitrate and sulphate precursors while releasing  $\text{HCl}(\text{g})$ , which then reacted with the incoming dust front. The segregation of sulphate from nitrate and chloride in individual dust particles is demonstrated for the first time. This is likely caused by the dust plume encountering elevated  $\text{SO}_2(\text{g})$  in the Chinese interior before reaching coastal urban areas polluted by both  $\text{SO}_2(\text{g})$  and  $\text{NO}_x(\text{g})$ . This caused the fractions of dust mixed with nitrate and/or chloride to be strongly dependent on the total dust loadings, whereas dust mixed with sulphate did not show this same dust concentration dependence. Ammonium was also significantly mixed with dust and the amount correlated strongly with the total amount of secondary acid reaction products in the dust. Submicron dust and ammonium sulphate were internally mixed, contrary to frequent statements that they exist as an external mixture. The size distribution of the mixing state of dust with these secondary species validates previous models and mechanisms of the atmospheric processing of dust. The uptake of secondary acids was also dependent on the individual dust particle mineralogy; nitrate accumulated on calcium-rich dust while sulphate accumulated on aluminosilicate-rich dust. Oxidation of S(IV) to S(VI) by iron in the aluminosilicate-rich dust is a probable explanation for this result, with important consequences for dust as a vector for the fertilization of remote oceans by soluble iron. This series of novel results has important implications for improving the treatment of dust in global chemistry models and highlights several key processes

## Processing of Asian dust

R. C. Sullivan et al.

Title Page

Abstract

Introduction

Conclusions

References

Tables

Figures

◀

▶

◀

▶

Back

Close

Full Screen / Esc

Printer-friendly Version

Interactive Discussion

requiring further investigation through laboratory and field studies.

## 1 Introduction

Major dust storm events typically develop in China in the spring, brought about by cold frontal systems and the Mongolian cyclonic depression (Sun et al., 2001). The Gobi Deserts in Mongolia and northern China, and the Taklimakan Desert in western China, are the two dominant source regions of dust in east Asia. Once lofted to high altitudes, dust can then become entrained in the jet stream and may be transported long distances over the Pacific Ocean to North America (Cahill, 2003; Darmenova et al., 2005; Duce et al., 1980; Jaffe et al., 1999; Thulasiraman et al., 2002; VanCuren, 2003). The Asian Pacific Regional Aerosol Characterization Experiment (ACE-Asia) in 2001 was designed to study the impact of these spring dust events on the physical, chemical and radiative properties of the Asian aerosol as it was transported over the mainland and the Pacific Ocean (Huebert et al., 2003; Seinfeld et al., 2004).

Mineral dust represents the second largest component of primary particle emissions by mass, with an estimated global source strength of 1000 to 3000 Mt/yr (Ginoux et al., 2001; Houghton et al., 2001). Laboratory studies have demonstrated the uptake of reactive gases including  $O_3$  (Chang et al., 2005; Hanisch and Crowley, 2003b; Michel et al., 2002; Sullivan et al., 2004; Usher et al., 2003b),  $NO_x$  (Grassian, 2002; Hanisch and Crowley, 2003a; Saliba et al., 2001),  $NO_y$  (e.g.  $HNO_3$ ,  $NO_3$ ,  $N_2O_5$ ) (Frinak et al., 2004; Krueger et al., 2004; Seisel et al., 2004, 2005; Underwood et al., 2001),  $SO_2$  (Al-Hosney and Grassian, 2005; Ullerstam et al., 2003, 2002; Usher et al., 2002), and organics (Al-Hosney et al., 2005; Carlos-Cuellar et al., 2003) on dust particles (Grassian, 2001; Usher et al., 2003a). Dust particles present a large surface area for heterogeneous reactions to occur on, and alter radiative transfer and rates of photolysis. Thus, dust influences the chemical composition of the troposphere, as demonstrated by numerous field and modeling studies (Bauer et al., 2004; Bian and Zender, 2003; de Reus et al., 2000, 2005; Dentener et al., 1996; Seinfeld et al., 2004; Tang et al., 2004a;

## Processing of Asian dust

R. C. Sullivan et al.

Title Page

Abstract

Introduction

Conclusions

References

Tables

Figures

◀

▶

◀

▶

Back

Close

Full Screen / Esc

Printer-friendly Version

Interactive Discussion

Zhang and Carmichael, 1999). Mineral dust particles can become internally mixed with secondary species such as ammonium sulphate, ammonium nitrate, hydrochloric acid, sea salt and biomass burning particles through coagulation, cloud processing, and heterogeneous reactions (Andreae et al., 1986; Clarke et al., 2004; Guazzotti et al., 2001a; Korhonen et al., 2003; Mamane and Gottlieb, 1989; Mori et al., 1998; Song and Carmichael, 1999; Wurzler et al., 2000; Yin et al., 2002; Zhang and Iwasaka, 2004; Zhang et al., 2003). These processes modify the chemical composition of the dust-laden aerosol and this can alter the radiative properties of the dust aerosol. The direct climate forcing of dust aerosol has a large reported range of  $-27.9$  to  $11.4 \text{ W cm}^{-2}$ ; differences in dust mineralogy and the atmospheric processing discussed above lead to these large uncertainties of the direct forcing (Houghton et al., 2001; Sokolik and Toon, 1996; Sokolik et al., 2001). The addition of water-soluble secondary species to a dust particle can alter its ability to act as a cloud or ice nucleus and thus influences the indirect climate forcing of dust (Cziczo et al., 2004; DeMott et al., 2003; Fan et al., 2004; Hung et al., 2003; Levin et al., 1996, 2005; Perry et al., 2004; Rudich et al., 2002; Wurzler et al., 2000; Yin et al., 2002). Photochemical processes and the uptake of secondary acids and organics can also increase the solubility and bioavailability of iron in dust particles, which is an important pathway for the fertilization of remote oceans with subsequent climate impacts (Bishop et al., 2002; Hand et al., 2004; Jickells et al., 2005; Meskhidze et al., 2005, 2003; Sarthou et al., 2003; Siefert et al., 1999; Turner and Hunter, 2001; Zhu et al., 1992, 1997). Mineral dust mixed with nitrate is also an important vector for nitrogen fertilization of oceans (Baker et al., 2003; Prospero and Savoie, 1989).

Asian mineral dust particles at their original source location are primarily composed of mixtures of quartz, clays, micas, feldspars, carbonates (primarily calcite,  $\text{CaCO}_3$ ), and other minor minerals (Gao and Anderson, 2001; Pye, 1987; Trochkin et al., 2003; Usher et al., 2003a; Yuan et al., 2004). The mineralogy of  $\text{PM}_{10}$  collected during severe Asian dust events in 2000 and 2002 in Beijing was determined by Shi et al. (2005) to be primarily clay minerals (>40%), followed by noncrystalline materials and quartz

**Processing of Asian dust**

R. C. Sullivan et al.

Title Page

Abstract

Introduction

Conclusions

References

Tables

Figures

◀

▶

◀

▶

Back

Close

Full Screen / Esc

Printer-friendly Version

Interactive Discussion

(both around 19%), with smaller amounts of calcite, plagioclase, K-feldspar, pyrite and other trace minerals. Surface measurements made in Beijing by Matsuki et al. (2005a) classified 28% of the Asian dust particles as calcite. The high carbonate fraction of Chinese dust is significant and this alkaline mineral has been shown to react readily with acidic species such as  $\text{HNO}_3$  to form  $\text{Ca}(\text{NO}_3)_2$  and liberate  $\text{CO}_2(\text{g})$  (Hanisch and Crowley, 2001; Johnson et al., 2005; Kelly and Wexler, 2005; Krueger et al., 2004; Laskin et al., 2005; Matsuki et al., 2005b; Song and Carmichael, 2001a).

In April 2001, a major dust storm event transported highly elevated levels of dust aerosol to the various ground, ship, and aircraft sampling platforms during ACE-Asia. The principal source regions of the dust during these events were the Taklimakan desert in Xinjiang Province and the desert regions in Mongolia, including the Gobi desert (Gong et al., 2003). Previous analyses of the dust storm aerosol produced a number of interesting and unique results. As the mineral dust aerosol was transported over China, Korea, and Japan to the ocean, it became mixed with anthropogenic, volcanic, and natural aerosols and aerosol precursor gases. When sampled onboard the R/V Ronald H. Brown in the Sea of Japan, the resulting aerosol was a complex mixture of mineral dust, organic carbon, elemental carbon, sulphates, nitrates, ammonium, and sea salt (Arimoto et al., 2006; Bates et al., 2004; Seinfeld et al., 2004). The high dust loading shifted the partitioning of much of the soluble material (e.g. nitrates, sulphates, organics) to the coarse mode aerosol ( $D_a > 1.0 \mu\text{m}$ ) from the accumulation mode ( $D_a 0.1\text{--}1.0 \mu\text{m}$ ), which decreased the soluble-ion content of the accumulation aerosol while negligibly changing the hygroscopicity of the coarse-dominated dust aerosol (Arimoto et al., 2006). Results obtained by an aerosol time-of-flight mass spectrometer (ATOFMS) revealed that prior to the dust front, the majority of supermicron particulate-nitrate was internally mixed with aged sea salt particles. After the dust front, the particulate-nitrate was found predominantly internally mixed with mineral dust particles (Bates et al., 2004; Tang et al., 2004b). ATOFMS results further demonstrated the significant uptake of chlorine by mineral dust particles during the dust event

---

**Processing of Asian dust**R. C. Sullivan et al.

---

[Title Page](#)[Abstract](#)[Introduction](#)[Conclusions](#)[References](#)[Tables](#)[Figures](#)[◀](#)[▶](#)[◀](#)[▶](#)[Back](#)[Close](#)[Full Screen / Esc](#)[Printer-friendly Version](#)[Interactive Discussion](#)

(Guazzotti et al., 2006<sup>1</sup>).

The results presented here further investigate the chemical aging of the mineral dust particles as mixing occurs with trace gases, and natural and anthropogenic aerosols. Our analysis provides new insights into the competitive uptake of different secondary acids by mineral dust and the role that the varying mineralogy of dust plays in these processes. These findings present yet another important dimension for models to consider when studying the atmospheric aging and radiative properties of mineral dust and further support the need to consider the importance of dust mineralogy (Krueger et al., 2004; Laskin et al., 2005; Matsuki et al., 2005a, b; Tang et al., 2004b).

## 2 Methods and instrumentation

A transportable aerosol time-of-flight mass spectrometer (ATOFMS) located on the R/V Ronald H. Brown (RHB) was used to help characterize the size and chemical composition of individual particles in real-time during the ACE-Asia campaign. The RHB left Hawaii on 16 March 2001 (DOY 75) and spent 10 days in transit to Japan. From DOY 90–99 the RHB circled around the southern end of Japan and into the Sea of Japan. On DOY 99 the RHB turned around and headed south out of the Sea of Japan through the Straits of Korea, finally docking at Yokosuka, Japan on DOY 110. More details on the RHB's cruise track and the air masses it sampled are available in Bates et al. (2004).

The aerosol sampled by the ATOFMS was drawn through a 6 m sample mast from ~18 m above sea level. The bottom 1.5 m of the mast was heated to maintain the relative humidity (*RH*) of the aerosol sample at  $55\pm 5\%$ . Air was only sampled when the relative wind speed and direction, and concentrations of particles larger than 15 nm,

<sup>1</sup> Guazzotti, S. A., Sullivan, R. C., Sodeman, D. A., Tang, Y. H., Carmichael, G. R., and Prather, K. A.: Mineral dust is a sink for chlorine in the marine boundary layer, Proc. Natl. Acad. Sci. USA, to be submitted, 2006.

Title Page

Abstract

Introduction

Conclusions

References

Tables

Figures

◀

▶

◀

▶

Back

Close

Full Screen / Esc

Printer-friendly Version

Interactive Discussion

indicated that the sampled air was free of local contamination (Bates et al., 2004).

The design and operation of the ATOFMS is described in detail elsewhere (Gard et al., 1997) and only a brief description is given here. The ATOFMS draws the aerosol sample through a converging nozzle into a differentially pumped vacuum chamber, accelerating each particle to its terminal velocity. The velocity of each particle is determined by the time-of-flight between two CW lasers. This velocity is converted to an aerodynamic diameter ( $D_a$ ) using a calibration curve generated with polystyrene latex spheres of discrete diameters. The particle's velocity also triggers the firing of a frequency-quadrupled Nd:YAG laser (266 nm) that desorbs and ionizes chemicals from each sized particle. A dual reflectron TOF-MS records the mass spectra of the resulting positive and negative ions simultaneously. The ATOFMS employed during ACE-Asia was capable of efficiently detecting particles between  $D_a$  0.2 and 3.0  $\mu\text{m}$ .

Analysis of the single-particle mass spectra was performed using the Matlab<sup>®</sup> based toolkit YAADA (<http://www.yaada.org>) to perform searches for particular mass spectral features within the dataset. An adaptive resonance theory-based neural network algorithm, ART-2a, was used to group the data into clusters of particles with similar mass spectral features, using a vigilance factor of 0.80 (Song et al., 1999). Measurements made by the ATOFMS have previously been used to monitor heterogeneous reactions occurring in sea-salt, mineral dust, and secondary organic aerosols, as well as in cloud droplets, in real-time (Angelino et al., 2001; Bates et al., 2004; Gard et al., 1998; Guazzotti et al., 2006<sup>1</sup>; Sullivan and Prather, 2005; Tang et al., 2004b; Whiteaker and Prather, 2003).

A wide variety of mineral dust samples from Asian desert regions were collected in 2001. Mass spectra from each dust sample were obtained by placing each dust sample into a flask in a sonicator to create a suspension of dust particles under nitrogen gas flow. The aerosol was then directed into the ATOFMS inlet for analysis and at least 2400 single-particle mass spectra were collected per sample.

---

**Processing of Asian dust**R. C. Sullivan et al.

---

Title Page

Abstract

Introduction

Conclusions

References

Tables

Figures

◀

▶

◀

▶

Back

Close

Full Screen / Esc

Printer-friendly Version

Interactive Discussion

### 3 Results

#### 3.1 Mineral dust mass spectra

The average mass spectrum for filtered mineral dust particles detected during the dust storm frontal passage (DOY 100.8–101.3) is shown in Fig. 1. The height of each peak indicates the fraction of particles that each that ion was detected in while the colour corresponds to the peak area range measured for that fraction of particles. Metals and metal oxides from minerals typical of dust particles are clearly evident in both the positive and negative ion spectra and their peak assignments are listed in Table 1, based on previous ATOFMS measurements (Guazzotti et al., 2001a, b; Pastor et al., 2003; Silva et al., 2000). Clearly these Asian dust particles are a complex mixture of numerous different minerals, as reported by previous studies (Andronova et al., 1993; Clarke et al., 2004; Gao and Anderson, 2001; Krueger et al., 2004; Pye, 1987; Trochkin et al., 2003; Usher et al., 2003a; Yuan et al., 2004).

The large fraction (>80%) of particles containing calcium marker ions ( $m/z$  +40, +56, +96) agrees with the high calcium carbonate fraction typical of Asian mineral dust. Krueger et al. (2004) reported the chemical composition of China Loess determined by EDX to be 39% Ca, 31% Si, 13% Mg, 7% Al, 4% Na, 3% Fe, and 1% K (atomic percent). The Ca component was determined to be mostly from carbonate minerals including calcite ( $\text{CaCO}_3$ ) and dolomite ( $\text{CaMg}(\text{CO}_3)_2$ ). The fraction of carbonate in Asian dust has been reported to range from 1–12% by mass (Andronova et al., 1993; Derbyshire et al., 1998; Nishikawa et al., 2000; Tang et al., 2004b). Carbonate is an enigmatic anion in mass spectrometry and is difficult to detect directly using a variety of ionization methods, including LAMMA (Bruynseels and Van Grieken, 1983), static SIMS (Shaw et al., 2003), and LDI (Silva et al., 2000). The counter-cation plays an important role in the detection of carbonate cluster ions; cation clusters from  $\text{Na}_2\text{CO}_3$  are readily created and detected but those from  $\text{CaCO}_3$  are not. The carbonate anion,  $\text{CO}_3^{-2}$ , generally has a low abundance in the mass spectrum and is obscured by the

[Title Page](#)[Abstract](#)[Introduction](#)[Conclusions](#)[References](#)[Tables](#)[Figures](#)[◀](#)[▶](#)[◀](#)[▶](#)[Back](#)[Close](#)[Full Screen / Esc](#)[Printer-friendly Version](#)[Interactive Discussion](#)

**Processing of Asian dust**

R. C. Sullivan et al.

Title Page

Abstract

Introduction

Conclusions

References

Tables

Figures

◀

▶

◀

▶

Back

Close

Full Screen / Esc

Printer-friendly Version

Interactive Discussion

more abundant isobars  $[\text{Si}_2\text{O}_2]^-$  and  $[\text{AlO}_2\text{H}]^-$  at  $m/z$  –60 in mineral particles. Thus, carbonate from calcite and dolomite cannot be directly determined using  $m/z$  –60. The presence of  $\text{CaCO}_3$  can be reliably inferred from Ca-containing cations including  $^{40}\text{Ca}^+$ ,  $^{56}[\text{CaO}]^+$ ,  $^{96}[\text{Ca}_2\text{O}]^+$ , and  $^{113}[(\text{CaO})_2\text{H}]^+$ . The  $^{56}[\text{CaO}]^+$  cation is likely formed via  $[\text{CaCO}_3]^+ \rightarrow [\text{CaO}]^+ + \text{CO}_2$ .

The intensity of a particular ion measured by ATOFMS is a function of the ability of the chemical matrix to absorb and distribute 266 nm radiation to the chemical constituents of the particle, as well as the ionization energy or electron affinity of the individual species (Gross et al., 2000). Na and K, for example, have very low ionization energies and thus typically produce very intense ion signals relative to other elements. Thus, the relative peak areas of various elements cannot be used to directly determine the relative amounts of different elements or compounds in a single-particle due to these varying sensitivities. If, however, the particle matrix is not changing significantly, as is the case for the Asian mineral dust particles discussed in this paper, then it is valid to compare the intensity of a particular peak from one particle to another and draw conclusions about the relative amounts of that specific species present in each particle.

The positive and in particular negative mass spectra also contain ions that correspond to ammonium, chloride, nitrate or sulphate. Table 1 lists these ions under “Secondary Species”. The principal ions used throughout this paper to study each of these four secondary species are indicated by an asterisk (\*) in Table 1. These peaks are used as evidence of the accumulation of secondary species by mineral dust, discussed below. In the source dust samples, some of these species could be present as minerals such as halite ( $\text{NaCl}$ ) and gypsum ( $\text{CaSO}_4$ ). Asian dust particles collected near their source typically have very low concentrations of sulphate, nitrate and chloride (Andronova et al., 1993; Arimoto et al., 2004; Mori et al., 2003; Nishikawa et al., 1991; Trochkin et al., 2003; Yuan et al., 2004; Zhang and Iwasaka, 1999).

Asian dust samples from various source regions were collected during ACE-Asia and analyzed by ATOFMS to create reference spectra of unprocessed dust. The spectra of source dust particles from regions such as Zhenbettai (Shaanxi Province, China), Dun-

huang (Gansu Province, China), and the CJ13 Certified Reference Asian Mineral Dust (Gansu Province, China) (Nishikawa et al., 2000) were collected (not shown) and compared to those of ambient mineral dust sampled during ACE-Asia, such as the spectra shown in Fig. 1. These represent likely sources of the mineral dust particles carried aloft from mainland China to the Sea of Japan during ACE-Asia (Gong et al., 2003). Similarities between mineral cations and anions for both source and ambient dust particles are readily evident. However, when compared to the ambient dust spectra, the source dust particles have much lower frequencies and ion intensities from secondary species such as ammonium, chloride, nitrate, and sulphate. Thus, the source dust spectra provide a benchmark for the very low background amounts of these species in Asian dust and allow us to attribute increases in the peak areas and detection frequencies from these secondary species to atmospheric processing during transport.

### 3.2 Filtering criteria

A total of 731 309 single-particle mass spectra were collected over the course of the campaign. From these 220 806 were classified as mineral dust particles after sorting by the ART-2a clustering algorithm (Song et al., 1999), based on the source dust mass spectra discussed above and those presented in Silva et al. (2000) and Guazzotti et al. (2001a).

Particles produced by biomass burning typically produce intense  $^{39}\text{K}^+$  signals, in addition to organic and elemental carbon fragments. The presence of large metal ion peaks such as  $^{39}\text{K}^+$  can cause biomass particles to be incorrectly placed in mineral dust clusters by the ART-2a algorithm. To correct for this, the mineral dust particles sorted by ART-2a were further filtered using a peak area  $^{27}\text{Al}^+ > 5000$  criteria to eliminate incorrectly sorted biomass particles. The  $^{27}\text{Al}^+$  criteria was chosen because Al is generally regarded as the most common single marker for mineral dust particles (Gao and Anderson, 2001; Mori et al., 2003; Nishikawa et al., 1991; Usher et al., 2003a) and is readily detected in mineral dust by ATOFMS (Guazzotti et al., 2001a; Silva et al., 2000). From previous source studies, we have determined that biomass particles do

## Processing of Asian dust

R. C. Sullivan et al.

Title Page

Abstract

Introduction

Conclusions

References

Tables

Figures

◀

▶

◀

▶

Back

Close

Full Screen / Esc

Printer-friendly Version

Interactive Discussion

not produce peak areas >5000 at  $m/z$  27 from  $^{27}[\text{C}_2\text{H}_3]^+$  or other organic fragments.

As dust particles are transported through the troposphere they can become internally mixed with other particle types such as sea salt, particularly via cloud processing if the dust aerosol passes through a cloudy region. Direct coagulation is also possible, but less likely, due to the slow diffusion times for these large particles. The fraction of mineral dust particles internally mixed with sea salt has been reported to be as high as 85% after transport through marine regions (Andreae et al., 1986; Fan et al., 1996; Niimura et al., 1998; Zhang and Iwasaka, 2004; Zhang et al., 2003). The mixing of dust and sea salt will alter the chemical composition of the mineral dust by adding significant amounts of sodium, chloride, sulphate and other ions. If the sea salt particle has already undergone heterogeneous aging by acids, then nitrate and non-sea-salt sulphate can also be incorporated into the mixed particle.

To focus only on the mixing of secondary acid products with mineral dust particles, the contributions of chloride, nitrate, and sulphate from internal mixing with sea salt must be excluded. Mineral dust particles that were internally mixed with sea salt were queried using a peak area >100 units for  $^{81}[\text{Na}_2^{35}\text{Cl}]^+$  criterion. The  $[\text{Na}_2\text{Cl}]^+$  ion is an ideal marker for various particle types internally mixed with sea salt (Guazzotti et al., 2001a) that was not present in the Asian dust source spectra. The final set of properly-calibrated dust particles that satisfied both the  $^{27}\text{Al}^+ > 5000$  and  $^{81}[\text{Na}_2^{35}\text{Cl}]^+ < 100$  peak area criteria will be herein referred to as “filtered dust particles”. Using this criterion, the fraction of mineral dust particles internally mixed with sea salt was determined to be  $15 \pm 9.5\%$  on average over the course of the entire study. Before the dust front the fraction of dust particles internally mixed with sea salt was as high as 40% (Guazzotti et al., 2006)<sup>1</sup>. While this degree of mixing is lower than previous single-particle filter-based measurements in this region (Fan et al., 1996; Zhang et al., 2003), a high degree of dust-sea salt mixing is typically caused by cloud processing. If the dust-laden air mass did not pass through a dense convective cloud system before reaching the RHB, this would explain the lower level of internal mixing. This may also be explained by the 0.2–3.0  $\mu\text{m}$  particle size range measured by the ATOFMS. The mixing of a dust particle

**Processing of Asian dust**

R. C. Sullivan et al.

Title Page

Abstract

Introduction

Conclusions

References

Tables

Figures

◀

▶

◀

▶

Back

Close

Full Screen / Esc

Printer-friendly Version

Interactive Discussion

**Processing of Asian dust**

R. C. Sullivan et al.

[Title Page](#)[Abstract](#)[Introduction](#)[Conclusions](#)[References](#)[Tables](#)[Figures](#)[◀](#)[▶](#)[◀](#)[▶](#)[Back](#)[Close](#)[Full Screen / Esc](#)[Printer-friendly Version](#)[Interactive Discussion](#)

EGU

with sea salt has been shown to increase the dust particle's diameter by  $\sim 0.4\text{--}0.8\ \mu\text{m}$  (Zhang and Iwasaka, 2004) and the peak in the number-weighted size distribution of mixed dust and sea salt particles is typically near or above  $3\ \mu\text{m}$  (Zhang et al., 2003). During the ACE-Asia dust event, the coarse-mode volume distribution peaked at  $\sim 4.0\ \mu\text{m}$  (Bates et al., 2004), implying that a large fraction of the internally mixed dust and sea-salt particles, if present, likely had diameters  $>3.0\ \mu\text{m}$  and were therefore not detected by ATOFMS.

Over the course of the campaign, the RHB sampled air arriving from a wide variety of source regions, as identified by Bates et al. (2004). We use the same source region classifications and time periods here. Mineral dust particles were commonly detected during the pre-frontal Marine and Polluted Korea & Japan time periods in low concentrations. From DOY 99.3–100.5 (UTC) the RHB sampled air that had passed over the Miyakejima volcano and Japan and a distinct dust layer was observed at an altitude of 5 km (Polluted Volcano time period). A major dust storm reached the RHB on DOY 100.8 in the western Sea of Japan (Dust Front time period). Upper level trajectories were from the north China/Mongolia desert region, while low-level trajectories extended across Korea and China. The passage of the front brought elevated levels of dust to the ship. The sub- $10\ \mu\text{m}$  dust concentrations reached  $140\ \mu\text{m m}^{-3}$  on DOY 102. From DOY 100 to 104 mineral dust composed 8–31% of submicron and up to 80% of supermicron mass (Arimoto et al., 2006). Dust continued to dominate the aerosol behind the front and from DOY 101.8–103.4 both upper and lower level trajectories crossed Korea and north China/Mongolia (Dust & Korea time period). From DOY 103.4–104.5 the RHB was in the Korean Strait and sampling air that came out of north China/Mongolia and had passed over Shanghai (Dust & Shanghai time period).

### 3.3 Detection of secondary species in dust particles

Nitrate, sulphate, and chloride were the most commonly observed anions in the mineral dust and correspond to the products expected from mineral dust particles that have mixed with secondary acids, as well as acid anhydrides including  $\text{N}_2\text{O}_5$ ,  $\text{SO}_2$ ,

**Processing of Asian dust**

R. C. Sullivan et al.

Title Page

Abstract

Introduction

Conclusions

References

Tables

Figures

◀

▶

◀

▶

Back

Close

Full Screen / Esc

Printer-friendly Version

Interactive Discussion

NO<sub>x</sub>, etc. Although the exact mechanism that leads to the accumulation of these secondary species cannot be determined from this data, the presence of chloride, nitrate, and sulphate on dust is most certainly due to the formation of hydrochloric, nitric, and sulphuric acids on the dust. This could be the result of reactive gases (e.g. SO<sub>2</sub>, NO<sub>2</sub>) adsorbing on the dust and then being oxidised to their acidic forms, or from the direct uptake of acidic gases (e.g. HCl, HNO<sub>3</sub>, H<sub>2</sub>SO<sub>4</sub>) or their ammonium salts (e.g. NH<sub>4</sub>NO<sub>3</sub>, (NH<sub>4</sub>)<sub>2</sub>SO<sub>4</sub>). After the acid is formed/adsorbed on the dust, it can be fully or partially neutralised by alkaline species in the dust (e.g. CaCO<sub>3</sub>) or by alkaline gases (e.g. NH<sub>3</sub>). The ions formed from these secondary species with ATOFMS cannot directly indicate if the species are acidic (i.e. protonated) or not. Therefore, we will refer to them as “secondary acid products” or simply “secondary acids” throughout our discussion, indicating that the chloride, nitrate, and sulphate found on the dust were most likely initially due to the formation/accumulation of secondary acids on the dust. The products of secondary species that reacted with mineral dust and other particle types are evaluated using the ions listed in Table 1. For this analysis chloride, nitrate, and sulphate were primarily determined using peaks at  $m/z$  –35, –62 and –97, respectively. The peak at <sup>62</sup>[NO<sub>3</sub>]<sup>–</sup> is used instead of the <sup>46</sup>[NO<sub>2</sub>]<sup>–</sup> nitrate fragment because  $m/z$  –62 is not detected in the Asian dust source spectra. Thus by using  $m/z$  –62 to detect nitrate in dust, we preclude any significant contribution from nitrate (or nitrite) that is already present in the dust before it is injected into the atmosphere. Recall that mixed dust-sea salt particles have also been filtered out.

The average mass spectrum for filtered mineral dust particles detected during the dust storm frontal passage (DOY 100.8–101.3) is shown in Fig. 1. Peaks typical of mineral dust particles discussed above and listed in Table 1 are clearly evident, and a large increase is observed in the fraction of particles producing ions indicative of secondary acid products including  $m/z$  +30, –35, –46, –62, –80, and –97. These secondary species peaks were not significantly present in the source dust spectra. Changes in the relative amounts of four secondary species in the mineral dust particles are evaluated by averaging the peak area ratio for each species from all filtered dust

particles detected in one hour, as shown in Fig. 2 for DOY 98–105, encompassing the prefrontal and postfrontal time periods. The peak area for a particular  $m/z$  is divided by that particle's peak area at  $m/z$  27 ( $\text{Al}^+$ ) to account for shot-to-shot variations in the LDI laser power and the amount of laser energy absorbed by each particle (Guazzotti et al., 2006<sup>1</sup>). The peak area ratio is evaluated for each individual particle before the hourly average is calculated. Al was chosen as a stable dust marker because it is the most commonly detected species in mineral dust by ATOFMS and has been shown to remain stable as a function of particle size during atmospheric transport (Guazzotti et al., 2001a; Mori et al., 2003; Silva et al., 2000).

### 3.4 Temporal evolution of secondary species in Asian dust

The principal peak area ratios for four major secondary species, ammonium, chloride, nitrate, and sulphate are plotted in Fig. 2. Gaps in the data occurred when aerosol sampling was suspended due to instrument maintenance or when the aerosol inlet was shut off during ship exhaust contamination periods. The total hourly ATOFMS dust particle counts are also displayed and indicate when the first dust front reached the RHB on DOY 100.8. Clear temporal changes in the relative amounts of the secondary species associated with the dust are evident.

To estimate the fraction of mineral dust particles internally mixed with chloride, nitrate, or sulphate, a peak area criterion  $>5000$  units for either  $^{35}\text{Cl}^-$ ,  $^{62}[\text{NO}_3]^-$  or  $^{97}[\text{HSO}_4]^-$  was used to define a mineral dust particle as significantly mixed with one of these secondary species. This peak area criterion was chosen because it is much larger than peak areas for these ions in the original Asian source dust and ensures that only mineral dust particles that have become significantly aged during transport will be selected. The mass fraction of each acid corresponding to a peak area of 5000 has not yet been determined and is the subject of ongoing laboratory studies. This peak area is relatively large and thus these results represent a conservative estimate of the degree to which mineral dust particles were internally mixed with nitrate, chloride, and/or sulphate. The results of this classification are shown in Fig. 3a for the prefrontal and

Title Page

Abstract

Introduction

Conclusions

References

Tables

Figures

◀

▶

◀

▶

Back

Close

Full Screen / Esc

Printer-friendly Version

Interactive Discussion

**Processing of Asian dust**

R. C. Sullivan et al.

[Title Page](#)[Abstract](#)[Introduction](#)[Conclusions](#)[References](#)[Tables](#)[Figures](#)[◀](#)[▶](#)[◀](#)[▶](#)[Back](#)[Close](#)[Full Screen / Esc](#)[Printer-friendly Version](#)[Interactive Discussion](#)

postfrontal periods. Large temporal changes in the fraction of reacted mineral dust particles are quite evident, similar to the temporal trends presented in Fig. 2. From DOY 98–105, the average ( $\pm 1\sigma$ ) fractions of dust particles mixed with nitrate, sulphate, or chloride were  $25.9\pm 9.6\%$ ,  $17.5\pm 8.5\%$ , and  $18.4\pm 10.5$ , respectively. These results differ from those we presented in Arimoto et al. (2006). In that paper we used the same criteria used here, but we did not exclude dust mixed with sea salt from the analysis so as to present a picture of the fraction of dust mixed with acids regardless of their source. Here we exclude dust internally mixed with sea salt to focus only on the role of secondary species, i.e. those produced in the atmosphere through chemical reactions.

The scatter plot shown in Fig. 3b (right) plots the hourly counts of dust mixed with one of the secondary species versus the total hourly dust counts measured by ATOFMS. Sulphate-dust has a very weak dependence on the total dust counts while nitrate-dust and chloride-dust have much stronger correlations over the DOY 98–105 time period. Thus, the mixing of dust with sulphate does not appear to be controlled by the total dust concentrations available, while the number of dust particles mixed with nitrate or chloride increases with increasing total dust concentrations.

### 3.5 Mixing state of secondary acids

Nitrate-dust and sulphate-dust together accounted for 13 754 particles from DOY 98–105, yet only 142 (1.03%) of these particles satisfied the peak area  $>5000$  criterion for both  $^{62}[\text{NO}_3]^-$  and  $^{97}[\text{HSO}_4]^-$ . Thus, significant amounts of both nitrate and sulphate did not accumulate on the same mineral dust particles. Similarly, only 98 out of 12 272 (0.80%) chloride-dust and sulphate-dust particles satisfied the peak area criteria for both  $^{35}\text{Cl}^-$  and  $^{97}\text{HSO}_4^-$ , demonstrating that secondary chloride and sulphate were also externally mixed in the mineral dust. Nitrate and chloride, however, were present in the same mineral dust particles to a large extent; 14.8% of chloride-dust and nitrate-dust particles had peak areas  $>5000$  for both  $^{35}\text{Cl}^-$  and  $^{62}\text{NO}_3^-$ . Recall that dust mixed with sea salt was excluded from this analysis and thus cannot account for this result.

The relative amounts of the three secondary species on all filtered dust particles

**Processing of Asian dust**

R. C. Sullivan et al.

Title Page

Abstract

Introduction

Conclusions

References

Tables

Figures

◀

▶

◀

▶

Back

Close

Full Screen / Esc

Printer-friendly Version

Interactive Discussion

classified as mixed (i.e. having a peak area  $>5000$  for  $m/z=-35$ ,  $-62$  or  $-97$ ) during two time periods are shown in Fig. 4. In the ternary plot, a dust particle containing primarily sulphate would appear at the top vertex, primarily nitrate at the right vertex, and primarily chloride at the left vertex. Particles that contain equal mixtures of all three species would be located in the centre while particles containing mixtures of only two of the acids would lie along one of the three axes. For both the Dust Front time period (Fig. 4a) and the pre-frontal Polluted Volcano time period (Fig. 4b), two broad groups of particles are evident in the ternary plots. The majority of particles lie along the bottom nitrate-chloride axis, indicating a wide range of internal mixing between nitrate and chloride in individual dust particles. A smaller but still substantial group of particles is found at the top sulphate vertex, indicating that these dust particles contain primarily sulphate and relatively little nitrate or chloride. The lack of a significant number of particles lying along the sulphate-chloride or sulphate-nitrate vertices, or found in the centre of the ternary plot, further demonstrates that sulphate in aged mineral dust particles is externally mixed from both nitrate and chloride. The colour of each point reflects that dust particle's absolute peak area for ammonium. Particles with the largest ammonium signals were found in dust particles also associated with nitrate or sulphate while chloride-dust particles had lower but still significant amounts of ammonium. The ternary plots of dust particles detected during the Polluted Volcano and Dust Front time periods share these general features but there are more particles from the sulphate-only group in the Polluted Volcano period and more in the nitrate-chloride group during the Dust Front period. This agrees with the temporal changes displayed in Figs. 2 and 3 that show a larger fraction of sulphate-dust before the dust front and a larger nitrate-dust and chloride-dust fraction during the dust storm.

This segregation of sulphate from nitrate and chloride is further demonstrated by the scatter plots (bottom) in Fig. 4a for the Dust Front time period. The ternary plots show the relative partitioning of the absolute peak area signals for each dust particle between the three major secondary acid peaks. The scatter plots, however, show the absolute areas for a set of two secondary acids for the same set of mixed filtered dust

particles used to generate the ternary plot. The large number of particles found along either axis in the sulphate-nitrate and sulphate-chloride scatter plots agrees with the segregation of sulphate from nitrate and chloride shown in the ternary plot. The large number of particles found near the centre of the nitrate-chloride scatter plot, however, further supports the substantial and variable internal mixing of these two secondary acids in the mineral dust. The reduced number of particles around the origin is caused by the peak area >5000 criterion for  $^{35}\text{Cl}^-$ ,  $^{62}\text{NO}_3^-$ , or  $^{97}\text{HSO}_4^-$ . Very similar results were also found for the Polluted Volcano time period (not shown).

### 3.6 Uptake of ammonia by acidified dust

Mineral dust that has accumulated secondary acids, as shown above, can be a sink for the principal alkaline gas in the atmosphere, ammonia. Figure 2 displays the  $\text{NH}_4/\text{Al}$  peak area ratio that represents the presence of ammonium in dust. By visual inspection of Fig. 2, there is already a clear correlation between the ammonium peak area ratio and that of nitrate, and to a lesser extent sulphate, and a strong anti-correlation with chloride. This suggests a strong association of ammonium with nitrate and sulphate in the aged mineral dust particles.

The presence of ammonium nitrate and/or ammonium sulphate in individual mineral dust particles is demonstrated in Fig. 5. The large cluster of particles lying along the ammonium-sulphate axis on the left indicates the presence of ammonium sulphate (AS) in mineral dust particles, while the smaller cluster of particles along the bottom ammonium-nitrate axis represents ammonium nitrate (AN) in dust. The fact that these particles appear primarily along one of these two axes indicates that the AS- or AN-dust particles do not also contain a significant nitrate or sulphate signal, respectively. This is expected based on the external mixing of nitrate and sulphate in dust presented above. The much larger spread in the ammonium sulphate dust particles along the ammonium-sulphate axis compared to the ammonium nitrate cluster may be due to the variable  $\text{NH}_4:\text{SO}_4$  molar ratio caused by partitioning between  $(\text{NH}_4)_2\text{SO}_4$ ,  $\text{NH}_4\text{HSO}_4$ , and  $\text{H}_2\text{SO}_4$ , which is controlled by the thermodynamic chemical equilibrium between

Title Page

Abstract

Introduction

Conclusions

References

Tables

Figures

◀

▶

◀

▶

Back

Close

Full Screen / Esc

Printer-friendly Version

Interactive Discussion

the particle-phase and the gas-phase (Stelson et al., 1979; Zhang et al., 2002). Similar patterns were found for the other time periods (not shown) with the relative amounts of ammonium nitrate and ammonium sulphate dust particles changing in response to the abundance of nitrate-dust and sulphate-dust, as presented above (Fig. 3).

To investigate if ammonium was only associated with dust particles which also contained nitrate, sulphate, or chloride, all filtered dust particles with a peak area >1000 for  $^{18}\text{[NH}_4\text{]}^+$  were queried, returning 8870 particles for DOY 98–105. 4208 of these were particles also mixed with nitrate, 1846 were in dust mixed with sulphate, and 1087 in dust mixed with chloride. Together dust mixed with one or more of the three acids accounted for 73% of the ammonium-containing dust. The remaining ammonium-dust particles can be explained by having significant signals for chloride, nitrate, and sulphate (i.e. peak area >1000) that did not exceed the 5000 peak area threshold. There were no indications in the average mass spectra that the ammonium was present in dust particles that did not also contain secondary acids to some extent. Therefore, ammonium was only found in dust particles that also contained acidic species such as nitric, sulphuric, and, to a lesser extent, hydrochloric acids.

As it is expected that a particle must first contain some acidic species in order for ammonia to partition to it, we would predict that the number of dust particles that contained ammonium would increase when the number of particles containing nitrate or sulphate increased. This would also be true if the mixing of dust with ammonium was caused by coagulation with or heterogeneous nucleation by ammonium nitrate/sulphate particles. This behaviour is shown in Fig. 6 for all filtered dust particles from DOY 98–105. A peak area >1000 for  $^{18}\text{[NH}_4\text{]}^+$  was used to classify a particle as mixed with ammonium and this search was performed within the subset of filtered dust particles previously classified as mixed with nitrate, sulphate, or chloride (“reacted dust particles”). The fraction of dust particles that contained ammonium tracked the temporal changes in the fractions of dust particles that were classified as mixed with either nitrate or sulphate above. The linear correlations between the hourly counts of dust that contained ammonium nitrate/sulphate and those that were mixed with nitrate/sulphate showed excellent

---

**Processing of Asian dust**R. C. Sullivan et al.

---

[Title Page](#)[Abstract](#)[Introduction](#)[Conclusions](#)[References](#)[Tables](#)[Figures](#)[◀](#)[▶](#)[◀](#)[▶](#)[Back](#)[Close](#)[Full Screen / Esc](#)[Printer-friendly Version](#)[Interactive Discussion](#)

**Processing of Asian dust**

R. C. Sullivan et al.

Title Page

Abstract

Introduction

Conclusions

References

Tables

Figures

◀

▶

◀

▶

Back

Close

Full Screen / Esc

Printer-friendly Version

Interactive Discussion

agreement with  $R^2=0.808$  and  $0.814$ , respectively (Fig. 6 insets). This is an impressive degree of correlation considering that these queries were performed on all reacted dust particles, regardless of mineralogy, for seven days of ambient sampling which included several changes in the air mass source regions. The slopes of these correlations indicate the average fraction of nitrate-dust or sulphate-dust particles which also contained ammonium over this time period were 43% and 32%, respectively. Note that the correlation for the AN-dust and nitrate-dust appears to have two slopes for unknown reasons. The temporal correlations of chloride-dust and dust mixed with both ammonium and chloride (not shown), thus containing ammonium chloride (AC), were not as significant as those for AS or AN. There were two time periods when AC-dust was detected and these both occurred when chloride-dust dominated. The largest of these was from DOY 101.88–102.38 at the beginning of the Dust & Korea time period when chloride-dust was also elevated (Fig. 3). During this short 13-h period, 29.8% of the 1087 total AC-dust particles were detected. During the Dust & Shanghai time period, from DOY 103.0–105.0, 52.4% of the total AC-dust particles were detected during this two day period. This coincided with a time when there were significant counts of chloride-, nitrate-, and sulphate-dust (Fig. 3). There were no significant counts of AC-dust during the first Dust Front time period (DOY 101) when the initial large increase in chloride-dust occurred.

Based on these observations the amount of ammonium in the dust particles would also be expected to track the amount of nitric or sulphuric acid available in the aged dust particles. Taking the sum of the nitrate ( $m/z=-62/27$ ) and sulphate ( $m/z=-97/27$ ) hourly peak area ratios as a measure of the available acid in the dust and plotting this versus ammonium ( $m/z=18/27$ ) in Fig. 7 reveals a strong temporal trend between the amount of acid in the dust and the amount of ammonium, as expected. Note the strong anti-correlation of ammonium and the two other acids with chloride ( $m/z=-35/27$ ) in the dust, particularly at DOY 101. However, from DOY 104–105 the peak area ratios for chloride, ammonium and the two acids all stabilize. The degree of correlation between the hourly peak area ratios for nitrate + sulphate, and ammonium has a  $R^2=0.574$  (not

shown). If the sum of the peak area ratios for all three acids is plotted versus that for ammonium as in Fig. 7 (bottom left), then the  $R^2$  is improved to 0.881. Considering that this correlation was evaluated for all the ambient filtered dust particles detected over seven days and a wide variety of air mass sources and that the different relative sensitivity factors for the various species have not yet been determined, this is an impressive degree of correlation. There is also a strong anti-correlation between the peak area ratio of chloride and ammonium (bottom right) with  $R^2=0.545$ . While including chloride in the sum of acid peak area ratios improved the overall correlation compared to just using the sum of nitrate + sulphate, chloride on its own is anti-correlated with ammonium in dust.

### 3.7 Effect of dust mineralogy on accumulation of secondary species

The role that dust particle mineralogy plays in its interactions with secondary acids and their precursors was investigated by comparing dust particles with significant Ca compared to dust with high amounts of Al. These types broadly represent dust particles rich in calcite or aluminosilicates, respectively. This was achieved by searching within the filtered dust for particles with a relative peak area  $>10\%$  for either  $^{27}\text{Al}^+$  or  $^{40}\text{Ca}^+$ . Together these two types of dust accounted for  $55.2\pm 5.7\%$  of the total filtered dust counts. Particles that were classified as both high in Ca and Al made up 9.4% of the total 19 400 high-Ca + high-Al filtered dust particles. Clear differences between these two types of dust can be seen in the temporal changes of the hourly peak area ratios for the three major secondary acid reaction products in Fig. 8. Most notable is a large spike in the sulphate area ratio at DOY 100.5 in the high-Al dust that does not occur in the high-Ca dust. The sulphate peak area ratio also increases from DOY 103.5–105 in the high-Al dust but remains mostly unchanged in the high-Ca dust. There are also noticeable differences in the increases in the chloride area ratio from DOY 101–102 for the two types of dust. The majority of chloride uptake during the Dust Front time period, beginning on DOY 100.8, took place on the high-Ca dust particles.

These results imply that sulphate is more strongly associated with aluminosilicate-

Title Page

Abstract

Introduction

Conclusions

References

Tables

Figures

◀

▶

◀

▶

Back

Close

Full Screen / Esc

Printer-friendly Version

Interactive Discussion

**Processing of Asian dust**

R. C. Sullivan et al.

Title Page

Abstract

Introduction

Conclusions

References

Tables

Figures

I◀

▶I

◀

▶

Back

Close

Full Screen / Esc

Printer-friendly Version

Interactive Discussion

rich dust particles while nitrate and chloride are more associated with calcite-rich dust. Further evidence for this mineralogy dependence is given in Fig. 9. The ternary plot displays the relative distribution of three major dust mineral components: aluminium, calcium, and iron. The  $^{54}\text{Fe}$  isotope was selected for iron to avoid interference from  $^{56}[\text{CaO}]^+$ . Filtered dust particles that were significantly mixed with at least one of the three secondary acids (i.e. peak area >5000) detected during the Dust & Shanghai time period are displayed in both Figs. 9a and b. In 9a, the symbol colour corresponds to the sulphate absolute peak area while in 9b, the colour corresponds to the nitrate absolute peak area. These two figures show dramatically different mixing behaviour for nitrate versus sulphate and are virtually complete opposites of each other, reflecting the segregation of nitrate from sulphate in dust particles, as discussed above. The sulphate-rich dust particles predominantly lie near the aluminium vertex and extend towards the iron vertex, indicating an association with aluminosilicate-dust particles. The nitrate-dust particles are mostly located towards the calcium vertex, being associated with calcite-rich dust. The processes that cause this behaviour are discussed below.

## 4 Discussion of results

### 4.1 Accumulation of secondary species in mineral dust during transport

From DOY 98 to 105, a substantial, though highly variable fraction of mineral dust was mixed with the secondary species chloride, nitrate, or sulphate. Previous analyses of Asian mineral dust particles near their source show they typically have low concentrations of nitrate, sulphate and chloride (Andronova et al., 1993; Arimoto et al., 2004; Matsuki et al., 2005a; Mori et al., 2003; Nishikawa et al., 1991; Trochkin et al., 2003; Yuan et al., 2004; Zhang and Iwasaka, 1999). Thus, we conclude that these mineral dust particles accumulated secondary acids as they were transported from the desert regions over the polluted mainland and marine regions to the RHB, by either direct heterogeneous uptake, cloud processing, or coagulation with other secondary-containing

**Processing of Asian dust**

R. C. Sullivan et al.

Title Page

Abstract

Introduction

Conclusions

References

Tables

Figures

I◀

▶I

◀

▶

Back

Close

Full Screen / Esc

Printer-friendly Version

Interactive Discussion

aerosols such as ammonium nitrate/sulphate particles. This is further confirmed by the temporal evolution of the relative amounts of the three acids in the dust, shown in Fig. 2. Just before the dust front, from DOY 100–100.8, there were elevated levels of both sulphate and ammonium corresponding to the Polluted Volcano air mass. From approximately DOY 100.8–102, the relative amount of chloride in the mineral dust increased dramatically, coinciding with the arrival of the dust front, while the amount of ammonium simultaneously decreased. The amount of nitrate and ammonium both increased noticeably from DOY 102–103.5. Dividing the peak areas of these species by a stable dust component, aluminium, provides further evidence of a secondary source for these four species. If these compounds were present in the dust particles at the source, we would expect their peak area ratios to remain constant as long as the dust source regions were not changing over short time periods. The fractions of dust mixed with secondary species (Fig. 3) show very similar temporal behaviour. There was a large increase in the fraction of dust mixed with sulphate on DOY 100.4 (Polluted Volcano time period), followed by a large increase in chloride-dust from DOY 100.8–101.3 (Dust Front time period). From DOY 102–103.5 (Dust & Korea time period), the fraction of nitrate-dust increased as chloride-dust decreased.

For some periods the changes in the fractions of dust mixed with one of the three secondary acids were reasonably well-correlated with another acid while at other times they were strongly anti-correlated. The degree to which the mineral dust became internally mixed with a particular acid is likely predominantly controlled by the air mass's history, and the availability of acidic vapours and their precursors in these air masses that then became associated with the mineral dust.

## 4.2 Segregation of sulphate from nitrate and chloride

To the best of our knowledge, this is the first report of the segregation of sulphate from nitrate and chloride in individual mineral dust particles that have experienced extensive atmospheric aging and transport (Fig. 4). These results were presented in a truncated form in Arimoto et al. (2006). Murphy and Thomson (1997) reported the

external mixture of chloride and sulphate in individual ambient particles (not limited to dust) detected at Idaho Hill and also found that sulphate and nitrate were usually, but not always, found in separate particles. Zhang et al. (2000) detected coarse and fine mode single particles collected on filters in coastal China that were internally mixed with sulphate and nitrate. These particles also typically contained mineral elements indicative of dust. Using similar methods, significant fractions of Asian dust particles collected in Japan were also found to contain both nitrate and sulphate (Zhang et al., 2003). In both these reports, the detection of nitrate and sulphate in each particle was purely qualitative and the detection limits for nitrate and sulphate on the coated collection substrates were  $10^{-14}$  and  $10^{-17}$  g, respectively. Thus, a mineral dust particle containing a very small amount of nitrate and/or sulphate would be reported as internally mixed with nitrate and sulphate.

Figure 3b shows that the degree of mixing of sulphate with dust is not strongly dependent on the total dust concentrations. The degree of mixing of nitrate and chloride with dust, however, does depend on the dust concentrations. This suggests that sulphate becomes preferentially mixed with dust, either because dust reacts with  $\text{SO}_2/\text{H}_2\text{SO}_4$  more efficiently, and/or because the dust plume encounters elevated sulphate precursors before encountering nitrate and chloride precursors. If dust mixes with sulphate first and becomes acidified then, in general, nitrate and chloride will only be able to become significantly mixed with dust if there are elevated dust concentrations such that there is an abundance of additional, mostly unreacted dust surface area available for reaction with nitrate and chloride precursors. There would therefore be a dependence on total dust loadings for nitrate- and chloride-dust, as shown in Fig. 3b.

Competition for the uptake of nitrate and sulphate by diesel exhaust particles was reported by Duran et al. (2003). They found that nitrate and sulphate were both present in the bulk diesel aerosol when the aerosol surface area was high. When the available surface area was reduced during high load engine modes, sulphates were selectively adsorbed by the soot. This indicates that sulphate (from  $\text{SO}_2$  oxidation) out-competes nitrate for adsorption onto soot particles. A similar competition may be occurring on

**Processing of Asian dust**

R. C. Sullivan et al.

Title Page

Abstract

Introduction

Conclusions

References

Tables

Figures

◀

▶

◀

▶

Back

Close

Full Screen / Esc

Printer-friendly Version

Interactive Discussion

mineral dust particles. Clearly, the very different physical and chemical nature of mineral dust and soot particles, in particular the alkalinity of Asian dust, must be considered here. Ooki and Uematsu (2005) reacted dust particles collected in Japan with  $\text{SO}_2$ ,  $\text{NO}_2$ ,  $\text{HNO}_3$  and HCl vapours. They found that  $\text{HNO}_3$  reacted more efficiently than  $\text{SO}_2$ , the opposite of what is shown herein and observed before, as discussed above. The important role of oxidants such as  $\text{O}_3$  for the oxidation of  $\text{SO}_2$  to sulphate in their experiments was not discussed, however. Zhang et al. (2003) concluded that the formation of sulphate on Asian dust is more efficient than for nitrate based on a much greater abundance of dust particles that contained sulphate than nitrate. They attributed this to the greater concentrations of  $\text{SO}_2$  than  $\text{NO}_x$  in East Asia and to the non-volatile nature of sulphuric acid compared to the more volatile nitric acid; we discuss both of these factors further below.

In addition to direct competition of  $\text{SO}_2$ ,  $\text{NO}_2$ ,  $\text{HNO}_3$ ,  $\text{NO}_y$ , HCl, etc. for reaction with fresh dust surfaces, the differing availability (i.e. vapour concentrations) of these aerosol precursors must be considered. As previously discussed, Asian dust is typically generated in the interior and then transported to the east towards the Pacific Ocean. In general, the emissions of  $\text{SO}_2$  are greater than of  $\text{NO}_x$  in east Asia. This difference is most pronounced in non-coastal areas due to  $\text{SO}_2$  emissions from industrial activity and coal power plants (Akimoto and Narita, 1994; Song and Carmichael, 2001b; Streets et al., 2003; Tang et al., 2004b). The emissions of  $\text{NO}_x$  are greatest in the large urban areas near the coast, but still do not exceed those of  $\text{SO}_2$ . Finally, the mixing ratios of HCl will be greatest in the polluted marine boundary layer primarily due to the release of HCl from acidified sea salt particles (Tang et al., 2004b). Thus it is reasonable to assume that mineral dust particles being transported eastward by a cold front first encounter elevated  $\text{SO}_2$ , followed by coastal regions polluted with both  $\text{SO}_2$  and  $\text{NO}_x$ , and finally elevated HCl once over marine areas. This causes sulphate to mix with dust first, before nitrate or chloride, and explains the weak dependence of sulphate-dust concentrations on the total dust loadings (Fig. 3b). This also explains why the formation of sulphate on dust had a higher affinity than for nitrate formation,

**Processing of Asian dust**

R. C. Sullivan et al.

Title Page

Abstract

Introduction

Conclusions

References

Tables

Figures

◀

▶

◀

▶

Back

Close

Full Screen / Esc

Printer-friendly Version

Interactive Discussion

despite the report by Ooki and Uematsu (2005) that  $\text{HNO}_3$  reacts with dust more efficiently than  $\text{SO}_2$  does. Changes in the emission inventories of Asia caused by the growing Chinese economy, as well as changes in technology and pollution controls, will likely alter this pattern of reactivity in the future.

#### 5 4.3 Mechanism of secondary acid uptake: size dependence

In general, the accumulation of sulphate by particles through reaction with  $\text{SO}_2/\text{H}_2\text{SO}_4$  is diffusion limited. Thus, it occurs preferentially in the particle size mode with the greatest surface area, which is typically the accumulation mode ( $D_a=0.1\text{--}1.0\ \mu\text{m}$ ) (Bassett and Seinfeld, 1984; Song and Carmichael, 1999). As sulphuric acid is essentially non-volatile and a stronger acid than both nitric or hydrochloric acid, the accumulation of sulphuric acid in a particle will displace these two more-volatile acids back to the gas-phase. Nitric acid and hydrochloric acid in the gas-phase can then re-partition to supermicron dust particles that have not already been acidified by sulphuric acid and which represent a larger alkaline sink by mass for the uptake of these acids (Bassett and Seinfeld, 1984; Song and Carmichael, 1999, 2001a). Thus, the irreversible uptake of  $\text{SO}_2$  and  $\text{H}_2\text{SO}_4$  is kinetically limited while the uptake of the more-volatile  $\text{HCl}$  and  $\text{HNO}_3$  is thermodynamically controlled. The uptake of ammonia is typically determined by the preceding  $\text{SO}_2/\text{H}_2\text{SO}_4$  uptake.

Evidence for this uptake mechanism occurring in the aged mineral dust detected during ACE-Asia is presented in the distribution of the peak areas for these secondary species as a function of particle size in Fig. 10a. The average peak areas for sulphate and ammonium clearly peak in the submicron filtered dust particles. Nitrate and chloride both peak in the supermicron dust particle mode. Despite the high loading of supermicron dust during the dust front, the largest aerosol surface area mode was still in the accumulation mode (Bates et al., 2004; Quinn et al., 2004). Similar results are shown in Fig. 10b, this time plotting the fraction of filtered dust particles previously classified as mixed with chloride, nitrate, sulphate (peak area  $>5000$ ), or ammonium (peak area  $>1000$ ) as a function of size. Again, sulphate-dust peaks in the submicron

Title Page

Abstract

Introduction

Conclusions

References

Tables

Figures

◀

▶

◀

▶

Back

Close

Full Screen / Esc

Printer-friendly Version

Interactive Discussion

**Processing of Asian dust**

R. C. Sullivan et al.

Title Page

Abstract

Introduction

Conclusions

References

Tables

Figures

◀

▶

◀

▶

Back

Close

Full Screen / Esc

Printer-friendly Version

Interactive Discussion

mode while nitrate- and chloride-dust peak in the supermicron. Ammonium-dust has two modes, the largest in the submicron mode along with sulphate-dust and a smaller one in the supermicron mode along with nitrate and chloride-dust. Taken together, these size plots indicate that ammonium accumulates in both the submicron sulphate-dust and the supermicron nitrate/chloride-dust, but the relative amount of ammonium per dust particle is greater in the submicron sulphate-dust mode.

Similar size-distributions of secondary species in Asian mineral dust have been reported previously from the analysis of collected filter samples and in modeling studies (Bates et al., 2004; Mori et al., 2003; Nishikawa et al., 1991; Ooki and Uematsu, 2005; Tang et al., 2004b; Wu and Okada, 1994; Zhang et al., 2000; Zhuang et al., 1999). However, our results are the first to show the size distribution of secondary species exclusively for individual aged mineral dust particles. We also have the ability to exclude the influence of internally mixed dust and sea salt particles. The  $0.10\ \mu\text{m}$  size resolution provided by the ATOFMS measurements is another significant advantage over filter-based methods. Together these factors result in a unique and important set of results that directly confirm aerosol model predictions of mineral dust aging mechanisms.

The displacement of nitrate and chloride caused by the uptake of  $\text{SO}_2/\text{H}_2\text{SO}_4$  is one explanation for the segregation of sulphate in mineral dust from nitrate and chloride in dust presented earlier in Fig. 4. Mineral dust that has accumulated enough  $\text{SO}_2/\text{H}_2\text{SO}_4$  to neutralize any alkaline components of the dust (likely  $\text{CaCO}_3$ ) and acidify the particle will also prevent any further uptake of nitric or hydrochloric acids by that dust particle. If uptake of sulphate versus nitrate and chloride were a displacement process, numerous dust particles should appear between the 100%  $\text{HSO}_4^-$  vertex and the 100%  $\text{NO}_3^-$  or 100%  $\text{Cl}^-$  vertex. Figure 4 clearly shows a lack of significant numbers of particles in these areas, indicating that competitive uptake of sulphate and the earlier mixing of dust with sulphate precursors were the likely causes of this segregation, not displacement. The chemical mineralogy of dust also plays an important role in determining which acids will preferentially react with dust. Together these processes explain the

**Processing of Asian dust**

R. C. Sullivan et al.

Title Page

Abstract

Introduction

Conclusions

References

Tables

Figures

◀

▶

◀

▶

Back

Close

Full Screen / Esc

Printer-friendly Version

Interactive Discussion

segregation of sulphate from nitrate and chloride in dust particles. The results suggest that the submicron dust particles were very acidic due to mixing with sulphuric acid. This prevented the substantial mixing of nitrate and chloride in the submicron dust particles. The internal mixing of nitrate and chloride is a result of the greater alkaline mass in the supermicron dust that can neutralize both acids and allow them to exist internally mixed to some degree in the same dust particle. The volatile nature of these two inorganic species allows them both to be displaced to the gas-phase, if this is occurring, and then re-partition back to the supermicron dust particles where they are less volatile. It is also possible that  $\text{HNO}_3$  could displace the more volatile chloride from mineral dust as  $\text{HCl}(\text{g})$ , analogous to its displacement from sea salt particles. As the uptake of  $\text{HCl}$  by mineral dust was only relatively recently reported (Guazzotti et al., 2006<sup>1</sup>; Ooki and Uematsu, 2005; Zhang and Iwasaka, 2001), this chemistry has only recently been incorporated into some thermodynamic models of mineral dust aging.

#### 4.4 Processes leading to the significant uptake of chloride by dust

As discussed by Guazzotti et al. (2006)<sup>1</sup>, the availability of  $\text{HCl}(\text{g})$  for reaction with the mineral dust was likely strongly influenced by the release of  $\text{SO}_2(\text{g})$  from the nearby Miyakejima volcano. Air masses sampled by the RHB showed a strong influence from the volcano from DOY 99–100.5 which corresponded to elevated  $[\text{SO}_2(\text{g})]$ , just before the dust front arrived at DOY 100.8 (Bates et al., 2004). Coinciding with this, the ratio of  $\text{SO}_4^{2-}$  to  $\text{NH}_4^+$  from filter measurements aboard the RHB showed elevated levels of particulate sulphate before the dust front, during the Polluted Volcano time period. In addition, previously reported ATOFMS results demonstrated that prior to the dust front the majority of nitrate- and sulphate-containing particles were acidified sea salt (Bates et al., 2004; Tang et al., 2004b). All of these results indicate that the sea salt particles in the prefrontal air mass were highly aged and resulted in a depletion of  $77 \pm 12\%$  of the total chloride available in the sea salt (Bates et al., 2004). Kajino et al. (2005) recently reported elevated concentrations of  $\text{HCl}(\text{g})$  and  $\text{HNO}_3(\text{g})$  in east Asia caused by the emission of  $\text{SO}_2(\text{g})$  from the Miyakejima volcano and the displacement

**Processing of Asian dust**

R. C. Sullivan et al.

Title Page

Abstract

Introduction

Conclusions

References

Tables

Figures

◀

▶

◀

▶

Back

Close

Full Screen / Esc

Printer-friendly Version

Interactive Discussion

EGU

of HCl(g) from sea salt particles acidified by SO<sub>2</sub>(g) uptake. Thus, there were likely elevated levels of HCl(g) in the marine boundary layer, caused by heterogeneous aging of sea salt particles, prior to the dust front. This liberated HCl(g) then mixed with the incoming dust front as it subsided while there were depleted levels of HNO<sub>3</sub>(g) and SO<sub>2</sub>/H<sub>2</sub>SO<sub>4</sub>(g), due to their prior reaction with sea salt, permitting substantial chloride uptake onto the mineral dust. As no measurements of HCl or nitrogen oxides were made during ACE-Asia, we must infer changes in the gas-phase composition from changes in the measured aerosol composition. Measurements during TRACE-P, just prior to and overlapping with ACE-Asia, found that the dominant forms of NO<sub>y</sub> in the region were HNO<sub>3</sub> and PAN (Talbot et al., 2003).

The lack of significant formation of sulphate and nitrate on mineral dust during the Dust Front time period is reflected in Figs. 2 and 3. These clearly show an increase in the amount of chloride in dust and a simultaneous decrease in the amount of nitrate and sulphate in dust during the dust front. This was likely caused by the prior uptake of sulphate and nitrate precursors on sea salt. The significant reaction of dust with HCl was also a result of the reduced concentrations of gas-phase nitrate and sulphate precursors. Had nitrate and/or sulphate formed on the dust particles during the dust front, this would have displaced much of the chloride to the gas-phase, or prevented its uptake in the first place. Thus, we hypothesize that the significant uptake of chloride by dust during the dust front occurred due to both the reduced mixing ratios of NO<sub>y</sub> and SO<sub>x</sub>, caused by their prior reaction with sea salt in the prefrontal air mass, and the subsequent release of HCl(g) from the highly aged sea salt particles.

#### 4.5 Internal mixtures of ammonium and mineral dust

Mineral dust can accumulate ammonium as a result of either direct uptake of ammonia from the gas-phase, coagulation with ammonium sulphate/nitrate-containing particles (Mori et al., 1998), or heterogeneous nucleation (Korhonen et al., 2003). In general, mineral dust shifts ammonia from the particle to gas phase by changing the aerosol from a cation- to anion-limited state due to the presence of alkaline species such as

calcium carbonate (Song and Carmichael, 1999; Tang et al., 2004b). Should dust become acidified by accumulating secondary acids and neutralise these alkaline species, as we have shown, the uptake of ammonia can occur. We have demonstrated that ammonium can become mixed with dust and that the amount of ammonium in the dust tracks the sum of the three acids very well (Figs. 6 and 7). In the troposphere, ammonium sulphate is the most stable and thus preferred ammonium salt. Ammonium nitrate is also commonly formed, and ammonium chloride, while the least preferred, is also a realistic ammonium salt in the troposphere. Indeed dust containing ammonium chloride was detected, as discussed previously. Thus, the amount of ammonium in dust should track the amount of chloride, in addition to sulphate and nitrate on dust. This should be especially true when the stronger sulphuric and nitric acids are not available to neutralise ammonia first, as was the case for the Dust Front time period. The best correlation for the amount of ammonium in dust was found by comparing this with the sum of the signals from chloride, nitrate, and sulphate (Fig. 7). This result was found despite the strong anti-correlation between the peak area ratio of chloride and ammonium. This could reflect the fact that AC-dust was only detected in two periods and at low concentrations, the first of which occurred when both sulphate-dust and nitrate-dust were greatly reduced. Thus, by including chloride, this time period of ammonium mixed with dust that would not be explained by sulphate or nitrate was captured. The overall anti-correlation of chloride and ammonium on dust may simply be a reflection of an anti-correlation of HCl(g) and NH<sub>3</sub>(g) mixing ratios, as the two likely have very different sources for this area. It does not necessarily reflect an inefficient process for ammonia to react with dust acidified by HCl. The concentrations of sulphate and nitrate precursors including SO<sub>x</sub>, NO<sub>x</sub>, and NO<sub>y</sub> were probably diminished during this period as well. The emission sources of ammonia are likely geographically similar to those of sulphur and nitrogen oxides, including the Miyakejima volcano and anthropogenic activities in general. Thus, changes in the air masses leading to decreased NO<sub>x</sub> and SO<sub>x</sub> likely also caused the NH<sub>3</sub> mixing ratios to decrease. The large SO<sub>2</sub>(g) emissions from the Miyakejima volcano were sufficient to exhaust all the volcanic NH<sub>3</sub>(g) emis-

**Processing of Asian dust**

R. C. Sullivan et al.

Title Page

Abstract

Introduction

Conclusions

References

Tables

Figures

◀

▶

◀

▶

Back

Close

Full Screen / Esc

Printer-friendly Version

Interactive Discussion

sions and still produce excess  $\text{H}_2\text{SO}_4$  (Kajino et al., 2005). This may have reduced the  $\text{NH}_3(\text{g})$  mixing ratios during the Dust Front time period, as we have already suggested that the dust front mixed with air influenced by the volcanic emissions prior to reaching the RHB.

5 The internal mixing of  $(\text{NH}_4)_2\text{SO}_4$ ,  $\text{NH}_4\text{NO}_3$ , and  $\text{NH}_4\text{Cl}$  with dust is a significant finding that has previously been reported from ATOFMS ambient measurements in Riverside, California (Noble and Prather, 1996), but not for dust storm events. Heterogeneous nucleation of  $(\text{NH}_4)_2\text{SO}_4$  on dust can produce ammonium sulphate coatings around dust and suppress the growth of ammonium sulphate particles to detectable  
10 sizes (Korhonen et al., 2003). Several researchers have frequently stated that ammonium sulphate measured in submicron particles during dust storms are due to ammonium sulphate particles externally mixed from dust (Jordan et al., 2003; Mori et al., 2003; Song and Carmichael, 2001b; Song et al., 2005; Tang et al., 2004b). We have clearly demonstrated that ammonium sulphate was internally mixed with dust particles  
15 during ACE-Asia, particularly in the submicron dust (Figs. 5 and 10). Thus, the assumption of externally mixed ammonium sulphate and dust particles during ACE-Asia at sea level was invalid and is likely incorrect in other locations as well. In the future, it would be worthwhile to consider this possibility when submicron ammonium sulphate is measured in the presence of elevated dust loadings; single particle measurements  
20 can be used to unambiguously determine the exact aerosol mixing state.

In Fig. 4, the dust particles with the largest ammonium signals were predominantly found in particles also mixed with sulphate (Fig. 4b, Polluted Volcano) or, with nitrate or sulphate (Fig. 4a, Dust Front). The latter result was somewhat unexpected as ammonium sulphate is the most stable, least volatile, and thus most preferred ammonium salt in the troposphere. The preference for  $\text{NH}_4\text{NO}_3$  in addition to  $(\text{NH}_4)_2\text{SO}_4$  is likely  
25 the result of a larger amount of nitrate-dust than sulphate-dust available for reaction with  $\text{NH}_3(\text{g})$  during this time period; Fig. 2 shows slightly elevated levels of nitrate-dust compared to sulphate-dust during the Dust Front. This could also have been caused by the heterogeneous nucleation and/or coagulation of  $\text{NH}_4\text{NO}_3$  on/with dust, as opposed

---

**Processing of Asian dust**R. C. Sullivan et al.

---

[Title Page](#)[Abstract](#)[Introduction](#)[Conclusions](#)[References](#)[Tables](#)[Figures](#)[◀](#)[▶](#)[◀](#)[▶](#)[Back](#)[Close](#)[Full Screen / Esc](#)[Printer-friendly Version](#)[Interactive Discussion](#)

to the dust first becoming mixed with nitric acid followed by neutralization by  $\text{NH}_3(\text{g})$ .

#### 4.6 Effect of mineralogy on mineral dust processing

Sulphate was highly associated with mineral dust rich in aluminosilicates and the associated enriched iron content (Jickells and Spokes, 2001), while nitrate was typically found in dust rich in calcium from calcite ( $\text{CaCO}_3$ ) or dolomite ( $\text{CaMg}(\text{CO}_3)_2$ ). The carbonate portion of Asian mineral dust is typically considered to be the principle component controlling the uptake of acidic vapours by dust due to its alkalinity (Song and Carmichael, 1999, 2001a; Tang et al., 2004b). If carbonate was the only dust component responsible for acid uptake, then we would expect to see sulphate also strongly associated with calcium-rich dust given that sulphate can displace other acids from dust particles and it is available for reaction with dust prior to the other acids, as outlined above. We propose that the association of sulphate with Al- and Fe-rich dust is due to the iron-catalyzed oxidation of  $\text{SO}_2$  to  $\text{H}_2\text{SO}_4$  (Brandt and Vaneldik, 1995; Finlayson-Pitts and Pitts, 2000; Qi et al., 2006; Rani et al., 1992; Yermakov and Purmal, 2003). The majority of the oxidation by this process is thought to occur in the aqueous phase containing the dissolved metal ions (i.e. a homogeneous reaction), but the role of surface-catalyzed heterogeneous reactions involving metals may also play an important role (Brandt and Vaneldik, 1995; Rani et al., 1992). The solubility of the metal ions is a key factor controlled by the aerosol's pH and the presence of organic compounds that could chelate the metals. The solubility of iron in dust aerosols is an important but poorly understood factor at present (Jickells et al., 2005; Jickells and Spokes, 2001; Luo et al., 2005). The rate of this reaction is accelerated at higher pH and thus this sulphate formation pathway is self-quenching. The alkaline nature of Asian mineral dust could enhance the role of iron in the oxidation of sulphur by buffering the pH and increasing this pathway's reaction rate compared to other major pathways such as oxidation by  $\text{H}_2\text{O}_2$ . A similar formation mechanism for nitrate involving Fe is not known which explains why nitrate is not associated with the Fe-rich aluminosilicate dust. Instead, nitrate became associated with Ca-rich dust through the neutralisation of

### Processing of Asian dust

R. C. Sullivan et al.

Title Page

Abstract

Introduction

Conclusions

References

Tables

Figures

◀

▶

◀

▶

Back

Close

Full Screen / Esc

Printer-friendly Version

Interactive Discussion

HNO<sub>3</sub> by carbonates. The role of relative humidity has been found to be an important factor for the uptake of acids by dust in both lab and recent field studies (Al-Hosney and Grassian, 2005; Goodman et al., 2001; Krueger et al., 2003; Laskin et al., 2005; Matsuki et al., 2005b; Ullerstam et al., 2002), however our data set does not allow us to directly investigate this important issue.

## 5 Atmospheric implications and conclusions

Single-particle ATOFMS measurements of dust particles during ACE-Asia show significant fractions of the dust were internally mixed with secondary acids and ammonium. To our knowledge, this is the first report of the segregation of sulphate from nitrate and chloride in individual dust particles. This was likely a result of the dust plume encountering elevated levels of sulphate precursors (e.g. SO<sub>2</sub>(g)) prior to nitrate precursors (e.g. NO<sub>x</sub>, HNO<sub>3</sub>), as the dust was transported towards the Pacific Ocean. Thus, the concentration of sulphate-dust was much less dependent on total dust particle concentrations than nitrate- or chloride-dust. The significant uptake of chloride (not from sea salt agglomeration) by dust from reaction with HCl(g) was caused by SO<sub>2</sub>(g) emissions from the Miyakejima volcano. The prior reaction of nitrate and sulphate precursors with sea salt particles reduced the availability for nitrate and sulphate to form on dust while simultaneously releasing HCl(g). Laboratory studies of the competitive reaction of various acidic gases with mineral dust particles are required to further investigate the novel segregation results reported here. This segregation and preferential temporal uptake of secondary acids has important implications for the accurate modeling of the troposphere's gas and particle phase composition during elevated dust loadings. This must be accounted for when modeling the evolution of dust particles during atmospheric transport and processing as it will affect the ability of aged dust to react further with trace gases.

Ammonium was only found in dust particles also containing secondary acids and the amount of ammonium in dust was strongly correlated with the sum of acids in the

Title Page

Abstract

Introduction

Conclusions

References

Tables

Figures

◀

▶

◀

▶

Back

Close

Full Screen / Esc

Printer-friendly Version

Interactive Discussion

**Processing of Asian dust**

R. C. Sullivan et al.

Title Page

Abstract

Introduction

Conclusions

References

Tables

Figures

◀

▶

◀

▶

Back

Close

Full Screen / Esc

Printer-friendly Version

Interactive Discussion

dust. Ammonium nitrate, ammonium sulphate, and ammonium chloride were internally mixed with dust particles including the submicron mode, contrary to previous suggestions that submicron ammonium sulphate is externally mixed from dust. Based on these findings, the common assumption that submicron ammonium sulphate and mineral dust particles are externally mixed should be revisited. Sulphate and ammonium were predominant in the submicron dust particles, while nitrate and chloride peaked in the supermicron dust. This provides direct evidence in support of modelled mechanisms of mineral dust aging, using single-particle measurements of size-segregated dust particles not mixed with sea salt to confirm these models' predictions.

The mixing of dust with secondary acids and ammonium has significant implications for the chemical composition of the troposphere, as well as the chemical, physical and optical properties of dust laden aerosol populations and their subsequent climactic effects. As has been previously discussed, the reaction of  $\text{NO}_y$  and  $\text{SO}_x$  species with dust can cause significant changes in the partitioning of trace reactive species between the gas and particle phase. The uptake of hydrochloric acid by mineral dust has recently been demonstrated in this and previous reports (Guazzotti et al., 2006<sup>1</sup>; Ooki and Uematsu, 2005; Zhang and Iwasaka, 2001) and must also be considered in models of tropospheric chemistry. Mixing of secondary acids and ammonium with supermicron-dominated dust in dust plumes causes a shift in the particulate loading of these species from submicron to supermicron particles. During ACE-Asia, this led to a decrease in the overall hygroscopicity of the aerosol population and removed aerosol mass from the optically efficient accumulation size mode (Arimoto et al., 2006; Carrico et al., 2003; Quinn et al., 2004). The addition of soluble material to dust can modify its CCN and IN ability, thus changing the cloud formation properties and lifetime of dust aerosols. Coating dust with secondary species can also alter the dust's direct radiative properties (Bauer and Koch, 2005; Conant et al., 2003).

During ACE-Asia, dust also scavenged semivolatile organic compounds, shifting them from the submicron to supermicron size range (Clarke et al., 2004). This had the interesting and important result of decreasing the scattering efficiency of the submicron

particles and thus increasing the absorption efficiency of the black carbon dominated submicron aerosol. The partitioning of sulphate and nitrate to supermicron-dominated dust had a similar effect. The internal mixing of dust particles with elemental and/or organic carbon (Clarke et al., 2004; Falkovich et al., 2004; Mace et al., 2003; Russell et al., 2002) is an important issue which we did not discuss here. Single-particle ATOFMS data on the internal mixing of dust with carbonaceous species can provide valuable insight into these processes and their consequences and will be the topic of a future manuscript.

By comparing the temporal evolution of secondary acids in dust particles of varying mineralogy, clear differences between high-Al and high-Ca dust particles were found. This is further evidence that mineralogy is an important parameter in dictating the reactions dust undergoes in the atmosphere. This could be due to different rates of reaction/formation of different acids with specific crustal minerals. The fact that the uptake of acids displayed a strong mineralogy dependence is further evidence for heterogeneous uptake of the acids. If the secondary acids had become mixed with the dust primarily through coagulation or heterogeneous nucleation, we would not expect such a strong dependence on the dust's mineralogy (Matsuki et al., 2005a). The effect of mineralogy deserves further attention in laboratory studies, particularly using authentic dust samples of varying composition. The dependence of the dust reactivity on its composition should also be incorporated into regional and global chemistry models (Krueger et al., 2004; Tang et al., 2004b).

Sulphate was highly associated with aluminosilicate- and iron-rich dust while nitrate combined with calcium-rich dust. The alkaline calcium carbonate neutralized nitric acid, leading to the accumulation of nitrate in calcium-rich dust. We propose that the sulphate association is due to the iron-catalyzed oxidation of S(IV) to S(VI) in the iron- and aluminosilicate-rich dust particles (Qi et al., 2006; Rani et al., 1992). This process has important implications for the fertilization of remote oceans and subsequent climate system feedbacks (Baker et al., 2003; Bishop et al., 2002; Duce, 1995; Jickells et al., 2005; Jickells and Spokes, 2001; Meskhidze et al., 2005). Iron is a key nu-

---

**Processing of Asian dust**R. C. Sullivan et al.

---

[Title Page](#)[Abstract](#)[Introduction](#)[Conclusions](#)[References](#)[Tables](#)[Figures](#)[I◀](#)[▶I](#)[◀](#)[▶](#)[Back](#)[Close](#)[Full Screen / Esc](#)[Printer-friendly Version](#)[Interactive Discussion](#)

**Processing of Asian dust**

R. C. Sullivan et al.

Title Page

Abstract

Introduction

Conclusions

References

Tables

Figures

◀

▶

◀

▶

Back

Close

Full Screen / Esc

Printer-friendly Version

Interactive Discussion

trient controlling biological productivity in high-nutrient low-chlorophyll (HNLC) ocean regions. Mineral dust that deposits in the oceans is the major source of iron to these remote regions (Duce and Tindale, 1991; Jickells and Spokes, 2001; Prospero and Savoie, 1989). However, it is believed that it is the amount of soluble iron in the dust particles, as opposed to the total iron content, which governs the fertilization of the oceans (Hand et al., 2004; Jickells et al., 2005; Luo et al., 2005; Meskhidze et al., 2003). The solubility of iron in dust particles can be increased as the particles become acidified by atmospheric processing and the accumulation of secondary acids (Zhu et al., 1992), such as has been shown extensively here. Submicron dust particles can be transported over further distances than larger dust particles due to their longer atmospheric lifetimes. Therefore the size distribution results we presented that demonstrate the accumulation of sulphate in submicron dust will have important implications for the transport of acidified dust particles containing soluble iron to remote ocean regions (Luo et al., 2005). Nitrate that has accumulated in mineral dust due to atmospheric processing is another important soluble nutrient for the oceans (Baker et al., 2003; Prospero and Savoie, 1989). The uptake and/or formation of organic compounds in the dust particles can also increase the iron's solubility if metal complexes are formed, with the oxalate anion for example, thus increasing their bioavailability (Meskhidze et al., 2003). These organic compounds may also inhibit or enhance the catalytic oxidation of sulphur compounds by iron (Siefert et al., 1994; Wolf et al., 2000; Zuo and Zhan, 2005).

Fertilization of HNLC ocean regions by soluble iron in dust increases ocean productivity, phytoplankton in particular, with a wide variety of climate feedbacks. For example, this could increase the uptake of carbon dioxide by marine organisms and also lead to increased DMS ocean emissions and thus increased cloud cover according to the CLAW hypothesis (Andreae et al., 1995; Charlson et al., 1987; Duce, 1995; Turner et al., 2004). The resulting climate changes (wind speeds and patterns, precipitation) can then affect the production and transport of aeolian crustal material to the oceans in the first place.

*Acknowledgements.* We thank I. Sokolik and her group for providing the Asian dust source samples and K. Coffee for collecting the source dust mass spectra. We thank V. Grassian and D. Murphy for valuable discussions regarding these results. Our participation in the ACE-Asia campaign was funded by the National Science Foundation.

## 5 References

Akimoto, H. and Narita, H.: Distribution Of SO<sub>2</sub>, NO<sub>x</sub> and CO<sub>2</sub> emissions from fuel combustion and industrial activities in Asia with 1-degrees- $\times$ 1-degrees resolution, *Atmos. Environ., Part A*, 28(2), 213–225, 1994.

Al-Hosney, H. A., Carlos-Cuellar, S., Baltrusaitis, J., and Grassian, V. H.: Heterogeneous uptake and reactivity of formic acid on calcium carbonate particles: a Knudsen cell reactor, FTIR and SEM study, *Phys. Chem. Chem. Phys.*, 7(20), 3587–3595, 2005.

Al-Hosney, H. A. and Grassian, V. H.: Water, sulfur dioxide and nitric acid adsorption on calcium carbonate: A transmission and ATR-FTIR study, *Phys. Chem. Chem. Phys.*, 7(6), 1266–1276, 2005.

Andreae, M. O., Charlson, R. J., Bruynseels, F., Storms, H., Vangrieken, R., and Maenhaut, W.: Internal mixture of sea salt, silicates, and excess sulfate in marine aerosols, *Science*, 232(4758), 1620–1623, 1986.

Andreae, M. O., Elbert, W., and Demora, S. J.: Biogenic sulfur emissions and aerosols over the tropical South-Atlantic. 3. Atmospheric dimethylsulfide, aerosols and cloud condensation nuclei, *J. Geophys Res.*, 100(D6), 11 335–11 356, 1995.

Andronova, A. V., Gomes, L., Smirnov, V. V., Ivanov, A. V., and Shukurova, L. M.: Physico-chemical characteristics of dust aerosols deposited during the Soviet-American experiment (Tajikistan, 1989), *Atmos. Environ., Part A*, 27(16), 2487–2493, 1993.

Angelino, S., Suess, D. T., and Prather, K. A.: Formation of aerosol particles from reactions of secondary and tertiary alkylamines: Characterization by aerosol time-of-flight mass spectrometry, *Environ. Sci. Technol.*, 35(15), 3130–3138, 2001.

Arimoto, R., Kim, Y. J., Kim, Y. P., Quinn, P. K., Bates, T. S., Anderson, T. L., Gong, S., Uno, I., Chin, M., Huebert, B. J., Clarke, A. D., Shinozuka, Y., Weber, R. J., Anderson, J. R., Guazzotti, S. A., Sullivan, R. C., Sodeman, D. A., Prather, K. A., and Sokolik, I. N.: Characterization of Asian Dust during ACE-Asia, *Global and Planetary Change*, in press, 2006.

## Processing of Asian dust

R. C. Sullivan et al.

Title Page

Abstract

Introduction

Conclusions

References

Tables

Figures

◀

▶

◀

▶

Back

Close

Full Screen / Esc

Printer-friendly Version

Interactive Discussion

**Processing of Asian dust**

R. C. Sullivan et al.

Title Page

Abstract

Introduction

Conclusions

References

Tables

Figures

◀

▶

◀

▶

Back

Close

Full Screen / Esc

Printer-friendly Version

Interactive Discussion

- Arimoto, R., Zhang, X. Y., Huebert, B. J., Kang, C. H., Savoie, D. L., Prospero, J. M., Sage, S. K., Schloesslin, C. A., Khaing, H. M., and Oh, S. N.: Chemical composition of atmospheric aerosols from Zhenbeitai, China, and Gosan, South Korea, during ACE-Asia, *J. Geophys. Res.*, 109(D19), doi:10.1029/2003JD004323, 2004.
- 5 Baker, A. R., Kelly, S. D., Biswas, K. F., Witt, M., and Jickells, T. D.: Atmospheric deposition of nutrients to the Atlantic Ocean, *Geophys. Res. Lett.*, 30(24), doi:10.1029/2003GL018518, 2003.
- Bassett, M. E. and Seinfeld, J. H.: Atmospheric equilibrium-model of sulfate and nitrate aerosols. 2. Particle-size analysis, *Atmos. Environ.*, 18(6), 1163–1170, 1984.
- 10 Bates, T. S., Quinn, P. K., Coffman, D. J., Covert, D. S., Miller, T. L., Johnson, J. E., Carmichael, G. R., Uno, I., Guazzotti, S. A., Sodeman, D. A., Prather, K. A., Rivera, M., Russell, L. M., and Merrill, J. T.: Marine boundary layer dust and pollutant transport associated with the passage of a frontal system over eastern Asia, *J. Geophys. Res.*, 109(D19), doi:10.1029/2003JD004094, 2004.
- 15 Bauer, S. E., Balkanski, Y., Schulz, M., Hauglustaine, D. A., and Dentener, F.: Global modeling of heterogeneous chemistry on mineral aerosol surfaces: Influence on tropospheric ozone chemistry and comparison to observations, *J. Geophys. Res.*, 109(D2), doi:10.1029/2003JD003868, 2004.
- Bauer, S. E. and Koch, D.: Impact of heterogeneous sulfate formation at mineral dust surfaces on aerosol loads and radiative forcing in the Goddard Institute for Space Studies general circulation model, *J. Geophys. Res.*, 110(D17), doi:10.1029/2005JD005870, 2005.
- Bian, H. S. and Zender, C. S.: Mineral dust and global tropospheric chemistry: Relative roles of photolysis and heterogeneous uptake, *J. Geophys. Res.*, 108(D21), doi:10.1029/2002JD003143, 2003.
- 25 Bishop, J. K. B., Davis, R. E., and Sherman, J. T.: Robotic observations of dust storm enhancement of carbon biomass in the North Pacific, *Science*, 298(5594), 817–821, 2002.
- Brandt, C. and Vaneldik, R.: Transition-metal-catalyzed oxidation of sulfur(IV) oxides – atmospheric-relevant processes and mechanisms, *Chemical Reviews*, 95(1), 119–190, 1995.
- 30 Bruynseels, F. J. and Van Grieken, R. E.: Molecular ion distributions in laser microprobe mass spectrometry of calcium oxide and calcium salts, *Spectrochim. Acta, Part B*, 38B(5–6), 853–858, 1983.
- Cahill, C. F.: Asian aerosol transport to Alaska during ACE-Asia, *J. Geophys. Res.*, 108(D23),

doi:10.1029/2002JD003271, 2003.

Carlos-Cuellar, S., Li, P., Christensen, A. P., Krueger, B. J., Burrichter, C., and Grassian, V. H.: Heterogeneous uptake kinetics of volatile organic compounds on oxide surfaces using a Knudsen cell reactor: Adsorption of acetic acid, formaldehyde, and methanol on alpha-Fe<sub>2</sub>O<sub>3</sub>, alpha-Al<sub>2</sub>O<sub>3</sub>, and SiO<sub>2</sub>, *J. Phys. Chem. A*, 107(21), 4250–4261, 2003.

Carrico, C. M., Kus, P., Rood, M. J., Quinn, P. K., and Bates, T. S.: Mixtures of pollution, dust, sea salt, and volcanic aerosol during ACE-Asia: Radiative properties as a function of relative humidity, *J. Geophys. Res.*, 108(D23), doi:10.1029/2003JD003405, 2003.

Chang, R. Y. W., Sullivan, R. C., and Abbatt, J. P. D.: Initial uptake of ozone on Saharan dust at atmospheric relative humidities, *Geophys. Res. Lett.*, 32(14), doi:10.1029/2005GL023317, 2005.

Charlson, R. J., Lovelock, J. E., Andreae, M. O., and Warren, S. G.: Oceanic phytoplankton, atmospheric sulfur, cloud albedo and climate, *Nature*, 326(6114), 655–661, 1987.

Clarke, A. D., Shinozuka, Y., Kapustin, V. N., Howell, S., Huebert, B., Doherty, S., Anderson, T., Covert, D., Anderson, J., Hua, X., Moore, K. G., McNaughton, C., Carmichael, G., and Weber, R.: Size distributions and mixtures of dust and black carbon aerosol in Asian outflow: Physiochemistry and optical properties, *J. Geophys. Res.*, 109(D15), doi:10.1029/2003JD004378, 2004.

Conant, W. C., Seinfeld, J. H., Wang, J., Carmichael, G. R., Tang, Y. H., Uno, I., Flatau, P. J., Markowicz, K. M., and Quinn, P. K.: A model for the radiative forcing during ACE-Asia derived from CIRPAS Twin Otter and R/V Ronald H. Brown data and comparison with observations, *J. Geophys. Res.*, 108(D23), doi:10.1029/2002JD003260, 2003.

Cziczo, D. J., Murphy, D. M., Hudson, P. K., and Thomson, D. S.: Single particle measurements of the chemical composition of cirrus ice residue during CRYSTAL-FACE, *J. Geophys. Res.*, 109(D4), doi:10.1029/2003JD004032, 2004.

Darmenova, K., Sokolik, I. N., and Darmenov, A.: Characterization of east Asian dust outbreaks in the spring of 2001 using ground-based and satellite data, *J. Geophys. Res.*, 110(D2), doi:10.1029/2004JD004842, 2005.

de Reus, M., Dentener, F., Thomas, A., Borrmann, S., Strom, J., and Lelieveld, J.: Airborne observations of dust aerosol over the North Atlantic Ocean during ACE 2: Indications for heterogeneous ozone destruction, *J. Geophys. Res.*, 105(D12), 15 263–15 275, 2000.

de Reus, M., Fischer, H., Sander, R., Gros, V., Kormann, R., Salisbury, G., Van Dingenen, R., Williams, J., Zollner, M., and Lelieveld, J.: Observations and model calculations of trace

ACPD

6, 4109–4170, 2006

## Processing of Asian dust

R. C. Sullivan et al.

Title Page

Abstract

Introduction

Conclusions

References

Tables

Figures

◀

▶

◀

▶

Back

Close

Full Screen / Esc

Printer-friendly Version

Interactive Discussion

EGU

gas scavenging in a dense Saharan dust plume during MINATROC, *Atmos. Chem. Phys.*, 5, 1787–1803, 2005.

DeMott, P. J., Sassen, K., Poellot, M. R., Baumgardner, D., Rogers, D. C., Brooks, S. D., Prenni, A. J., and Kreidenweis, S. M.: African dust aerosols as atmospheric ice nuclei, *Geophys. Res. Lett.*, 30(14), doi:10.1029/2003GL017410, 2003.

Dentener, F. J., Carmichael, G. R., Zhang, Y., Lelieveld, J., and Crutzen, P. J.: Role of mineral aerosol as a reactive surface in the global troposphere, *J. Geophys. Res.*, 101(D17), 22 869–22 889, 1996.

Derbyshire, E., Meng, X. M., and Kemp, R. A.: Provenance, transport and characteristics of modern aeolian dust in western Gansu Province, China, and interpretation of the Quaternary loess record, *J. Arid Environ.*, 39(3), 497–516, 1998.

Duce, R. A.: Sources, distributions, and fluxes of mineral aerosols and their relationship to climate, in: *Aerosol forcing of climate*, edited by: Charlson, R. J. and Heintzenberg, J., John Wiley & Sons Ltd., Chichester, England, 1995.

Duce, R. A. and Tindale, N. W.: Atmospheric transport of iron and its deposition in the ocean, *Limnol. Oceanogr.*, 36(8), 1715–1726, 1991.

Duce, R. A., Unni, C. K., Ray, B. J., Prospero, J. M., and Merrill, J. T.: Long-range atmospheric transport of soil dust from Asia to the tropical North Pacific – temporal variability, *Science*, 209(4464), 1522–1524, 1980.

Duran, A., Carmona, M., and Ballesteros, R.: Competitive diesel engine emissions of sulphur and nitrogen species, *Chemosphere*, 52(10), 1819–1823, 2003.

Falkovich, A. H., Schkolnik, G., Ganor, E., and Rudich, Y.: Adsorption of organic compounds pertinent to urban environments onto mineral dust particles, *J. Geophys. Res.*, 109(D2), doi:10.1029/2003JD003919, 2004.

Fan, S. M., Horowitz, L. W., Levy, H., and Moxim, W. J.: Impact of air pollution on wet deposition of mineral dust aerosols, *Geophys. Res. Lett.*, 31(2), doi:10.1029/2003GL018501, 2004.

Fan, X. B., Okada, K., Niimura, N., Kai, K., Arao, K., Shi, G. Y., Qin, Y., and Mitsuta, Y.: Mineral particles collected in China and Japan during the same Asian dust-storm event, *Atmos. Environ.*, 30(2), 347–351, 1996.

Finlayson-Pitts, B. J. and Pitts, J. N.: *Chemistry of the upper and lower atmosphere: Theory, experiments, and applications*, Academic Press, San Diego, 2000.

Frinak, E. K., Wermeille, S. J., Mashburn, C. D., Tolbert, M. A., and Pursell, C. J.: Heterogeneous reaction of gaseous nitric acid on gamma-phase iron(III) oxide, *J. Phys. Chem. A*,

**Processing of Asian dust**

R. C. Sullivan et al.

Title Page

Abstract

Introduction

Conclusions

References

Tables

Figures

◀

▶

◀

▶

Back

Close

Full Screen / Esc

Printer-friendly Version

Interactive Discussion

108(9), 1560–1566, 2004.

Gao, Y. and Anderson, J. R.: Characteristics of Chinese aerosols determined by individual-particle analysis, *J. Geophys. Res.*, 106(D16), 18 037–18 045, 2001.

Gard, E., Mayer, J. E., Morrical, B. D., Dienes, T., Fergenson, D. P., and Prather, K. A.: Real-time analysis of individual atmospheric aerosol particles: Design and performance of a portable ATOFMS, *Anal. Chem.*, 69(20), 4083–4091, 1997.

Gard, E. E., Kleeman, M. J., Gross, D. S., Hughes, L. S., Allen, J. O., Morrical, B. D., Fergenson, D. P., Dienes, T., Galli, M. E., Johnson, R. J., Cass, G. R., and Prather, K. A.: Direct observation of heterogeneous chemistry in the atmosphere, *Science*, 279(5354), 1184–1187, 1998.

Ginoux, P., Chin, M., Tegen, I., Prospero, J. M., Holben, B., Dubovik, O., and Lin, S. J.: Sources and distributions of dust aerosols simulated with the GOCART model, *J. Geophys. Res.-Atmos.*, 106(D17), 20 255–20 273, 2001.

Gong, S. L., Zhang, X. Y., Zhao, T. L., McKendry, I. G., Jaffe, D. A., and Lu, N. M.: Characterization of soil dust aerosol in China and its transport and distribution during 2001 ACE-Asia: 2. Model simulation and validation, *J. Geophys. Res.*, 108(D9), doi:10.1029/2002JD002633, 2003.

Goodman, A. L., Bernard, E. T., and Grassian, V. H.: Spectroscopic study of nitric acid and water adsorption on oxide particles: Enhanced nitric acid uptake kinetics in the presence of adsorbed water, *J. Phys. Chem. A*, 105(26), 6443–6457, 2001.

Grassian, V. H.: Heterogeneous uptake and reaction of nitrogen oxides and volatile organic compounds on the surface of atmospheric particles including oxides, carbonates, soot and mineral dust: implications for the chemical balance of the troposphere, *Int. Rev. Phys. Chem.*, 20(3), 467–548, 2001.

Grassian, V. H.: Chemical reactions of nitrogen oxides on the surface of oxide, carbonate, soot, and mineral dust particles: Implications for the chemical balance of the troposphere, *J. Phys. Chem. A*, 106(6), 860–877, 2002.

Gross, D. S., Galli, M. E., Silva, P. J., and Prather, K. A.: Relative sensitivity factors for alkali metal and ammonium cations in single particle aerosol time-of-flight mass spectra, *Anal. Chem.*, 72 (2), 416-422, 2000.

Guazzotti, S. A., Coffee, K. R., and Prather, K. A.: Continuous measurements of size-resolved particle chemistry during INDOEX-Intensive Field Phase 99, *J. Geophys. Res.*, 106(D22), 28 607–28 627, 2001a.

Guazzotti, S. A., Whiteaker, J. R., Suess, D., Coffee, K. R., and Prather, K. A.: Real-time

**Processing of Asian dust**

R. C. Sullivan et al.

Title Page

Abstract

Introduction

Conclusions

References

Tables

Figures

◀

▶

◀

▶

Back

Close

Full Screen / Esc

Printer-friendly Version

Interactive Discussion

**Processing of Asian dust**

R. C. Sullivan et al.

Title Page

Abstract

Introduction

Conclusions

References

Tables

Figures

◀

▶

◀

▶

Back

Close

Full Screen / Esc

Printer-friendly Version

Interactive Discussion

measurements of the chemical composition of size-resolved particles during a Santa Ana wind episode, California USA, *Atmos. Environ.*, 35(19), 3229–3240, 2001b.

Hand, J. L., Mahowald, N. M., Chen, Y., Siefert, R. L., Luo, C., Subramaniam, A., and Fung, I.: Estimates of atmospheric-processed soluble iron from observations and a global mineral aerosol model: Biogeochemical implications, *J. Geophys. Res.*, 109(D17), doi:10.1029/2004JD004574, 2004.

Hanisch, F. and Crowley, J. N.: Heterogeneous reactivity of gaseous nitric acid on  $\text{Al}_2\text{O}_3$ ,  $\text{CaCO}_3$ , and atmospheric dust samples: A Knudsen cell study, *J. Phys. Chem. A*, 105(13), 3096–3106, 2001.

Hanisch, F. and Crowley, J. N.: Heterogeneous reactivity of NO and  $\text{HNO}_3$  on mineral dust in the presence of ozone, *Phys. Chem. Chem. Phys.*, 5(5), 883–887, 2003a.

Hanisch, F. and Crowley, J. N.: Ozone decomposition on Saharan dust: an experimental investigation, *Atmos. Chem. Phys.*, 3, 119–130, 2003b.

Houghton, J. T., Ding, Y., Griggs, D. J., Noguer, M., van der Linden, P. J., Dai, X., Maskell, K., and Johnson, C. A.: *Climate Change 2001: The Scientific Basis*, Cambridge University Press, Cambridge, 2001.

Huebert, B. J., Bates, T., Russell, P. B., Shi, G. Y., Kim, Y. J., Kawamura, K., Carmichael, G., and Nakajima, T.: An overview of ACE-Asia: Strategies for quantifying the relationships between Asian aerosols and their climatic impacts, *J. Geophys. Res.*, 108(D23), doi:10.1029/2003JD003550, 2003.

Hung, H. M., Malinowski, A., and Martin, S. T.: Kinetics of heterogeneous ice nucleation on the surfaces of mineral dust cores inserted into aqueous ammonium sulfate particles, *J. Phys. Chem. A*, 107(9), 1296–1306, 2003.

Jaffe, D., Anderson, T., Covert, D., Kotchenruther, R., Trost, B., Danielson, J., Simpson, W., Berntsen, T., Karlsdottir, S., Blake, D., Harris, J., Carmichael, G., and Uno, I.: Transport of Asian air pollution to North America, *Geophys. Res. Lett.*, 26(6), 711–714, 1999.

Jickells, T. D., An, Z. S., Andersen, K. K., Baker, A. R., Bergametti, G., Brooks, N., Cao, J. J., Boyd, P. W., Duce, R. A., Hunter, K. A., Kawahata, H., Kubilay, N., laRoche, J., Liss, P. S., Mahowald, N., Prospero, J. M., Ridgwell, A. J., Tegen, I., and Torres, R.: Global iron connections between desert dust, ocean biogeochemistry, and climate, *Science*, 308(5718), 67–71, 2005.

Jickells, T. D. and Spokes, L. J.: Atmospheric iron inputs to the oceans, in: *The biogeochemistry of iron in seawater*, edited by: Turner, D. R. and Hunter, K. A., John Wiley & Sons Ltd.,

Chichester, England, 2001.

Johnson, E. R., Sciegienka, J., Carlos-Cuellar, S., and Grassian, V. H.: Heterogeneous uptake of gaseous nitric acid on dolomite ( $\text{CaMg}(\text{CO}_3)_2$ ) and calcite ( $\text{CaCO}_3$ ) particles: A knudsen cell study using multiple, single, and fractional particle layers, *J. Phys. Chem. A*, 109(31), 6901–6911, 2005.

Jordan, C. E., Dibb, J. E., Anderson, B. E., and Fuelberg, H. E.: Uptake of nitrate and sulfate on dust aerosols during TRACE-P, *J. Geophys. Res.*, 108(D21), 1–10, 2003.

Kajino, M., Ueda, H., Satsumabayashi, H., and Han, Z. W.: Increase in nitrate and chloride deposition in east Asia due to increased sulfate associated with the eruption of Miyakejima Volcano, *J. Geophys. Res.*, 110(D18), doi:10.1029/2005JD005879, 2005.

Kelly, J. T. and Wexler, A. S.: Thermodynamics of carbonates and hydrates related to heterogeneous reactions involving mineral aerosol, *J. Geophys. Res.*, 110(D11), doi:10.1029/2004JD005583, 2005.

Korhonen, H., Napari, I., Timmreck, C., Vehkamäki, H., Pirjola, L., Lehtinen, K. E. J., Lauri, A., and Kulmala, M.: Heterogeneous nucleation as a potential sulphate-coating mechanism of atmospheric mineral dust particles and implications of coated dust on new particle formation, *J. Geophys. Res.*, 108(D17), doi:10.1029/2003JD003553, 2003.

Krueger, B. J., Grassian, V. H., Cowin, J. P., and Laskin, A.: Heterogeneous chemistry of individual mineral dust particles from different dust source regions: the importance of particle mineralogy, *Atmos. Environ.*, 38(36), 6253–6261, 2004.

Krueger, B. J., Grassian, V. H., Laskin, A., and Cowin, J. P.: The transformation of solid atmospheric particles into liquid droplets through heterogeneous chemistry: Laboratory insights into the processing of calcium containing mineral dust aerosol in the troposphere, *Geophys. Res. Lett.*, 30(3), doi:10.1029/2002GL016563, 2003.

Laskin, A., Iedema, M. J., Ichkovich, A., Graber, E. R., Taraniuk, I., and Rudich, Y.: Direct observation of completely processed calcium carbonate dust particles, *Faraday Discuss.*, 130, 453–468, 2005.

Levin, Z., Ganor, E., and Gladstein, V.: The effects of desert particles coated with sulfate on rain formation in the eastern Mediterranean, *J. Appl. Meteorol.*, 35(9), 1511–1523, 1996.

Levin, Z., Teller, A., Ganor, E., and Yin, Y.: On the interactions of mineral dust, sea-salt particles, and clouds: A measurement and modeling study from the Mediterranean Israeli Dust Experiment campaign, *J. Geophys. Res.*, 110(D20), doi:10.1029/2005JD005810, 2005.

Luo, C., Mahowald, N. M., Meskhidze, N., Chen, Y., Siefert, R. L., Baker, A. R., and Johansen,

Processing of Asian dust

R. C. Sullivan et al.

Title Page

Abstract

Introduction

Conclusions

References

Tables

Figures

◀

▶

◀

▶

Back

Close

Full Screen / Esc

Printer-friendly Version

Interactive Discussion

**Processing of Asian dust**

R. C. Sullivan et al.

Title Page

Abstract

Introduction

Conclusions

References

Tables

Figures

◀

▶

◀

▶

Back

Close

Full Screen / Esc

Printer-friendly Version

Interactive Discussion

A. M.: Estimation of iron solubility from observations and a global aerosol model, *J. Geophys. Res.*, 110(D23), doi:10.1029/2005JD006059, 2005.

Mace, K. A., Kubilay, N., and Duce, R. A.: Organic nitrogen in rain and aerosol in the eastern Mediterranean atmosphere: An association with atmospheric dust, *J. Geophys. Res.*, 108(D10), doi:10.1029/2002JD002997, 2003.

Mamane, Y. and Gottlieb, J.: Heterogeneous reactions of minerals with sulfur and nitrogen oxides, *J. Aerosol Sci.*, 20(3), 303–311, 1989.

Matsuki, A., Iwasaka, Y., Shi, G. Y., Chen, H. B., Osada, K., Zhang, D., Kido, M., Inomata, Y., Kim, Y. S., Trochkin, D., Nishita, C., Yamada, M., Nagatani, T., Nagatani, M., and Nakata, H.: Heterogeneous sulfate formation on dust surface and its dependence on mineralogy: Balloon-borne observations from balloon-borne measurements in the surface of Beijing, China, *Water, Air, and Soil Pollution: Focus*, 5, 101–132, 2005a.

Matsuki, A., Iwasaka, Y., Shi, G. Y., Zhang, D. Z., Trochkin, D., Yamada, M., Kim, Y. S., Chen, B., Nagatani, T., Miyazawa, T., Nagatani, M., and Nakata, H.: Morphological and chemical modification of mineral dust: Observational insight into the heterogeneous uptake of acidic gases, *Geophys. Res. Lett.*, 32(22), doi:10.1029/2005GL024176, 2005b.

Meskhidze, N., Chameides, W. L., and Nenes, A.: Dust and pollution: A recipe for enhanced ocean fertilization?, *J. Geophys. Res.*, 110(D3), doi:10.1029/2004JD005082, 2005.

Meskhidze, N., Chameides, W. L., Nenes, A., and Chen, G.: Iron mobilization in mineral dust: Can anthropogenic SO<sub>2</sub> emissions affect ocean productivity?, *Geophys. Res. Lett.*, 30(21), doi:10.1029/2003GL018035, 2003.

Michel, A. E., Usher, C. R., and Grassian, V. H.: Heterogeneous and catalytic uptake of ozone on mineral oxides and dusts: A Knudsen cell investigation, *Geophys. Res. Lett.*, 29(14), doi:10.1029/2002GL014896, 2002.

Mori, I., Nishikawa, M., and Iwasaka, Y.: Chemical reaction during the coagulation of ammonium sulphate and mineral particles in the atmosphere, *Sci. Total Environ.*, 224(1–3), 87–91, 1998.

Mori, I., Nishikawa, M., Tanimura, T., and Quan, H.: Change in size distribution and chemical composition of kosa (Asian dust) aerosol during long-range transport, *Atmos. Environ.*, 37(30), 4253–4263, 2003.

Murphy, D. M. and Thomson, D. S.: Chemical composition of single aerosol particles at Idaho Hill: Negative ion measurements, *J. Geophys. Res.*, 102(D5), 6353–6368, 1997.

Niimura, N., Okada, K., Fan, X. B., Kai, K., Arao, K., Shi, G. Y., and Takahashi, S.: Formation

**Processing of Asian dust**

R. C. Sullivan et al.

Title Page

Abstract

Introduction

Conclusions

References

Tables

Figures

◀

▶

◀

▶

Back

Close

Full Screen / Esc

Printer-friendly Version

Interactive Discussion

- of Asian dust-storm particles mixed internally with sea salt in the atmosphere, *J. Meteorol. Soc. Japan*, 76(2), 275–288, 1998.
- Nishikawa, M., Hao, Q., and Morita, M.: Preparation and evaluation of certified reference materials for asian mineral dust, *Global Environ. Res.*, 4(1), 103–113, 2000.
- 5 Nishikawa, M., Kanamori, S., Kanamori, N., and Mizoguchi, T.: Kosa aerosol as eolian carrier of anthropogenic material, *Sci. Total Environ.*, 107, 13–27, 1991.
- Noble, C. A. and Prather, K. A.: Real-time measurement of correlated size and composition profiles of individual atmospheric aerosol particles, *Environ. Sci. Technol.*, 30(9), 2667–2680, 1996.
- 10 Ooki, A. and Uematsu, M.: Chemical interactions between mineral dust particles and acid gases during Asian dust events, *J. Geophys. Res.*, 110(D3), doi:10.1029/2004JD004737, 2005.
- Pastor, S. H., Allen, J. O., Hughes, L. S., Bhave, P., Cass, G. R., and Prather, K. A.: Ambient single particle analysis in Riverside, California by aerosol time-of-flight mass spectrometry during the SCOS97-NARSTO, *Atmos. Environ.*, 37, S239–S258, 2003.
- 15 Perry, K. D., Cliff, S. S., and Jimenez-Cruz, M. P.: Evidence for hygroscopic mineral dust particles from the Intercontinental Transport and Chemical Transformation Experiment, *J. Geophys. Res.*, 109(D23), doi:10.1029/2004JD004979, 2004.
- Prospero, J. M. and Savoie, D. L.: Effect of continental sources on nitrate concentrations over the Pacific-Ocean, *Nature*, 339(6227), 687–689, 1989.
- Pye, K.: *Aeolian dusts and dust deposits*, Academic Press, San Diego, 1987.
- Qi, J., Feng, L., Li, X., and Zhang, M.: An X-ray photoelectron spectroscopy study of elements on the surface of aerosol particles, *J. Aerosol Sci.*, 37(2), 218–227, 2006.
- Quinn, P. K., Coffman, D. J., Bates, T. S., Welton, E. J., Covert, D. S., Miller, T. L., Johnson, J. E., Maria, S., Russell, L., Arimoto, R., Carrico, C. M., Rood, M. J., and Anderson, J.: Aerosol optical properties measured on board the Ronald H. Brown during ACE-Asia as a function of aerosol chemical composition and source region, *J. Geophys. Res.*, 109(D19), doi:10.1029/2003JD004010, 2004.
- 25 Rani, A., Prasad, D. S. N., Madhawat, P. V. S., and Gupta, K. S.: The role of free-fall atmospheric dust in catalyzing autoxidation of aqueous sulfur-dioxide, *Atmos. Environ., Part A*, 26(4), 667–673, 1992.
- 30 Rudich, Y., Khersonsky, O., and Rosenfeld, D.: Treating clouds with a grain of salt, *Geophys. Res. Lett.*, 29(22), doi:10.1029/2002GL016055, 2002.

**Processing of Asian dust**

R. C. Sullivan et al.

Title Page

Abstract

Introduction

Conclusions

References

Tables

Figures

◀

▶

◀

▶

Back

Close

Full Screen / Esc

Printer-friendly Version

Interactive Discussion

- Russell, L. M., Maria, S. F., and Myneni, S. C. B.: Mapping organic coatings on atmospheric particles, *Geophys. Res. Lett.*, 29(16), doi:10.1029/2002GL014874, 2002.
- Saliba, N. A., Yang, H., and Finlayson-Pitts, B. J.: Reaction of gaseous nitric oxide with nitric acid on silica surfaces in the presence of water at room temperature, *J. Phys. Chem. A*, 105(45), 10339–10346, 2001.
- 5 Sarthou, G., Baker, A. R., Blain, S., Achterberg, E. P., Boye, M., Bowie, A. R., Croot, P., Laan, P., de Baar, H. J. W., Jickells, T. D., and Worsfold, P. J.: Atmospheric iron deposition and sea-surface dissolved iron concentrations in the eastern Atlantic Ocean, *Deep-Sea Res. Part I – Oceanographic Research Papers*, 50(10–11), 1339–1352, 2003.
- 10 Seinfeld, J. H., Carmichael, G. R., Arimoto, R., Conant, W. C., Brechtel, F. J., Bates, T. S., Cahill, T. A., Clarke, A. D., Doherty, S. J., Flatau, P. J., Huebert, B. J., Kim, J., Markowicz, K. M., Quinn, P. K., Russell, L. M., Russell, P. B., Shimizu, A., Shinzuka, Y., Song, C. H., Tang, Y. H., Uno, I., Vogelmann, A. M., Weber, R. J., Woo, J. H., and Zhang, X. Y.: ACE-ASIA - Regional climatic and atmospheric chemical effects of Asian dust and pollution, *Bull. Amer. Meteorol. Soc.*, 85(3), 367–380, 2004.
- 15 Seisel, S., Borensen, C., Vogt, R., and Zellner, R.: The heterogeneous reaction of HNO<sub>3</sub> on mineral dust and gamma-alumina surfaces: a combined Knudsen cell and DRIFTS study, *Phys. Chem. Chem. Phys.*, 6(24), 5498–5508, 2004.
- Seisel, S., Borensen, C., Vogt, R., and Zellner, R.: Kinetics and mechanism of the uptake of N<sub>2</sub>O<sub>5</sub> on mineral dust at 298 K, *Atmos. Chem. Phys.*, 5, 3423–3432, 2005.
- 20 Shaw, A. D., Cortez, M. M., Gianotto, A. K., Appelhans, A. D., Olson, J. E., Karahan, C., Avci, R., and Groenewold, G. S.: Static SIMS analysis of carbonate on basic alkali-bearing surfaces, *Surf. Interface Anal.*, 35(3), 310–317, 2003.
- Shi, Z. B., Shao, L. T., Jones, T. P., and Lu, S. L.: Microscopy and mineralogy of airborne particles collected during severe dust storm episodes in Beijing, China, *J. Geophys. Res.*, 110(D1), doi:10.1029/2004JD005073, 2005.
- 25 Siefert, R. L., Johansen, A. M., and Hoffmann, M. R.: Chemical characterization of ambient aerosol collected during the southwest monsoon and intermonsoon seasons over the Arabian Sea: Labile-Fe(II) and other trace metals, *J. Geophys. Res.*, 104(D3), 3511–3526, 1999.
- 30 Siefert, R. L., Pehkonen, S. O., Erel, Y., and Hoffmann, M. R.: Iron photochemistry of aqueous suspensions of ambient aerosol with added organic-acids, *Geochim. Cosmochim. Acta*, 58(15), 3271–3279, 1994.

**Processing of Asian dust**

R. C. Sullivan et al.

Title Page

Abstract

Introduction

Conclusions

References

Tables

Figures

◀

▶

◀

▶

Back

Close

Full Screen / Esc

Printer-friendly Version

Interactive Discussion

- Silva, P. J., Carlin, R. A., and Prather, K. A.: Single particle analysis of suspended soil dust from Southern California, *Atmos. Environ.*, 34(11), 1811–1820, 2000.
- Sokolik, I. N. and Toon, O. B.: Direct radiative forcing by anthropogenic airborne mineral aerosols, *Nature*, 381(6584), 681–683, 1996.
- 5 Sokolik, I. N., Winker, D. M., Bergametti, G., Gillette, D. A., Carmichael, G., Kaufman, Y. J., Gomes, L., Schuetz, L., and Penner, J. E.: Introduction to special section: Outstanding problems in quantifying the radiative impacts of mineral dust, *J. Geophys. Res.*, 106(D16), 18 015–18 027, 2001.
- Song, C. H. and Carmichael, G. R.: The aging process of naturally emitted aerosol (sea-salt and mineral aerosol) during long range transport, *Atmos. Environ.*, 33(14), 2203–2218, 1999.
- Song, C. H. and Carmichael, G. R.: Gas-particle partitioning of nitric acid modulated by alkaline aerosol, *J. Atmos. Chem.*, 40(1), 1–22, 2001a.
- Song, C. H. and Carmichael, G. R.: A three-dimensional modeling investigation of the evolution processes of dust and sea-salt particles in east Asia, *J. Geophys Res.*, 106(D16), 18 131–18 154, 2001b.
- 15 Song, C. H., Maxwell-Meier, K., Weber, R. J., Kapustin, V., and Clarke, A.: Dust composition and mixing state inferred from airborne composition measurements during ACE-Asia C130 Flight #6, *Atmos. Environ.*, 39(2), 359–369, 2005.
- Song, X. H., Hopke, P. K., Fergenson, D. P., and Prather, K. A.: Classification of single particles analyzed by ATOFMS using an artificial neural network, ART-2A, *Anal. Chem.*, 71(4), 860–865, 1999.
- 20 Stelson, A. W., Friedlander, S. K., and Seinfeld, J. H.: Note on the equilibrium relationship between ammonia and nitric-acid and particulate ammonium-nitrate, *Atmos. Environ.*, 13(3), 369–371, 1979.
- Streets, D. G., Bond, T. C., Carmichael, G. R., Fernandes, S. D., Fu, Q., He, D., Klimont, Z., Nelson, S. M., Tsai, N. Y., Wang, M. Q., Woo, J. H., and Yarber, K. F.: An inventory of gaseous and primary aerosol emissions in Asia in the year 2000, *J. Geophys Res.*, 108(D21), doi:10.1029/2002JD003093, 2003.
- 30 Sullivan, R. C. and Prather, K. A.: Recent advances in our understanding of atmospheric chemistry and climate made possible by on-line aerosol analysis instrumentation, *Anal. Chem.*, 77(12), 3861–3885, 2005.
- Sullivan, R. C., Thornberry, T., and Abbatt, J. P. D.: Ozone decomposition kinetics on alumina:

effects of ozone partial pressure, relative humidity and repeated oxidation cycles, *Atmos. Chem. Phys.*, 4, 1301–1310, 2004.

Sun, J. M., Zhang, M. Y., and Liu, T. S.: Spatial and temporal characteristics of dust storms in China and its surrounding regions, 1960-1999: Relations to source area and climate, *J. Geophys. Res.*, 106(D10), 10 325–10 333, 2001.

Talbot, R., Dibb, J., Scheuer, E., Seid, G., Russo, R., Sandholm, S., Tan, D., Singh, H., Blake, D., Blake, N., Atlas, E., Sachse, G., Jordan, C., and Avery, M.: Reactive nitrogen in Asian continental outflow over the western Pacific: Results from the NASA Transport and Chemical Evolution over the Pacific (TRACE-P) airborne mission, *J. Geophys. Res.*, 108(D20), doi:10.1029/2002JD003129, 2003.

Tang, Y. H., Carmichael, G. R., Kurata, G., Uno, I., Weber, R. J., Song, C. H., Guttikunda, S. K., Woo, J. H., Streets, D. G., Wei, C., Clarke, A. D., Huebert, B., and Anderson, T. L.: Impacts of dust on regional tropospheric chemistry during the ACE-Asia experiment: A model study with observations, *J. Geophys. Res.*, 109(D19), doi:10.1029/2003JD003806, 2004a.

Tang, Y. H., Carmichael, G. R., Seinfeld, J. H., Dabdub, D., Weber, R. J., Huebert, B., Clarke, A. D., Guazzotti, S. A., Sodeman, D. A., Prather, K. A., Uno, I., Woo, J. H., Yienger, J. J., Streets, D. G., Quinn, P. K., Johnson, J. E., Song, C. H., Grassian, V. H., Sandu, A., Talbot, R. W., and Dibb, J. E.: Three-dimensional simulations of inorganic aerosol distributions in east Asia during spring 2001, *J. Geophys. Res.*, 109(D19), doi:10.1029/2003JD004201, 2004b.

Thulasiraman, S., O'Neill, N. T., Royer, A., Holben, B. N., Westphal, D. L., and McArthur, L. J. B.: Sunphotometric observations of the 2001 Asian dust storm over Canada and the US, *Geophys. Res. Lett.*, 29(8), doi:10.1029/2001GL014188, 2002.

Trochikine, D., Iwasaka, Y., Matsuki, A., Yamada, M., Kim, Y. S., Nagatani, T., Zhang, D., Shi, G. Y., and Shen, Z.: Mineral aerosol particles collected in Dunhuang, China, and their comparison with chemically modified particles collected over Japan, *J. Geophys. Res.*, 108(D23), doi:10.1029/2002JD003268, 2003.

Turner, D. R. and Hunter, K. A.: *The biogeochemistry of iron in seawater*, John Wiley & Sons Ltd., Chichester, England, 2001.

Turner, S. M., Harvey, M. J., Law, C. S., Nightingale, P. D., and Liss, P. S.: Iron-induced changes in oceanic sulfur biogeochemistry, *Geophys. Res. Lett.*, 31(14), doi:10.1029/2004GL020296, 2004.

Ullerstam, M., Johnson, M. S., Vogt, R., and Ljungstrom, E.: DRIFTS and Knudsen cell study of the heterogeneous reactivity of SO<sub>2</sub> and NO<sub>2</sub> on mineral dust, *Atmos. Chem. Phys.*, 3,

**Processing of Asian dust**

R. C. Sullivan et al.

Title Page

Abstract

Introduction

Conclusions

References

Tables

Figures

◀

▶

◀

▶

Back

Close

Full Screen / Esc

Printer-friendly Version

Interactive Discussion

2043–2051, 2003.

Ullerstam, M., Vogt, R., Langer, S., and Ljungstrom, E.: The kinetics and mechanism of SO<sub>2</sub> oxidation by O<sub>3</sub> on mineral dust, *Phys. Chem. Chem. Phys.*, 4(19), 4694–4699, 2002.

Underwood, G. M., Li, P., Al-Abadleh, H., and Grassian, V. H.: A Knudsen cell study of the heterogeneous reactivity of nitric acid on oxide and mineral dust particles, *J. Phys. Chem. A*, 105(27), 6609–6620, 2001.

Usher, C. R., Al-Hosney, H., Carlos-Cuellar, S., and Grassian, V. H.: A laboratory study of the heterogeneous uptake and oxidation of sulfur dioxide on mineral dust particles, *J. Geophys. Res.*, 107(D23), doi:10.1029/2002JD002051, 2002.

Usher, C. R., Michel, A. E., and Grassian, V. H.: Reactions on mineral dust, *Chem. Rev.*, 103(12), 4883–4939, 2003a.

Usher, C. R., Michel, A. E., Stec, D., and Grassian, V. H.: Laboratory studies of ozone uptake on processed mineral dust, *Atmos. Environ.*, 37(38), 5337–5347, 2003b.

VanCuren, R. A.: Asian aerosols in North America: Extracting the chemical composition and mass concentration of the Asian continental aerosol plume from long-term aerosol records in the western United States, *J. Geophys. Res.*, 108(D20), doi:10.1029/2003JD003459, 2003.

Whiteaker, J. R. and Prather, K. A.: Hydroxymethanesulfonate as a tracer for fog processing of individual aerosol particles, *Atmos. Environ.*, 37(8), 1033–1043, 2003.

Wolf, A., Deutsch, F., Hoffmann, P., and Ortner, H. M.: The influence of oxalate on Fe-catalyzed S(IV) oxidation by oxygen in aqueous solution, *J. Atmos. Chem.*, 37(2), 125–135, 2000.

Wu, P. M. and Okada, K.: Nature of coarse nitrate particles in the atmosphere – A single, particle approach, *Atmos. Environ.*, 28(12), 2053–2060, 1994.

Wurzler, S., Reisin, T. G., and Levin, Z.: Modification of mineral dust particles by cloud processing and subsequent effects on drop size distributions, *J. Geophys. Res.*, 105(D4), 4501–4512, 2000.

Yermakov, A. N. and Purmal, A. P.: Iron-catalyzed oxidation of sulfite: From established results to a new understanding, *Progress In Reaction Kinetics And Mechanism*, 28(3), 189–255, 2003.

Yin, Y., Wurzler, S., Levin, Z., and Reisin, T. G.: Interactions of mineral dust particles and clouds: Effects on precipitation and cloud optical properties, *J. Geophys. Res.*, 107(D23), doi:10.1029/2001JD001544, 2002.

Yuan, H., Rahn, K. A., and Zhuang, G.: Graphical techniques for interpreting the composition of individual aerosol particles, *Atmos. Environ.*, 38(39), 6845–6854, 2004.

ACPD

6, 4109–4170, 2006

## Processing of Asian dust

R. C. Sullivan et al.

Title Page

Abstract

Introduction

Conclusions

References

Tables

Figures

◀

▶

◀

▶

Back

Close

Full Screen / Esc

Printer-friendly Version

Interactive Discussion

EGU

**Processing of Asian dust**

R. C. Sullivan et al.

Title Page

Abstract

Introduction

Conclusions

References

Tables

Figures

◀

▶

◀

▶

Back

Close

Full Screen / Esc

Printer-friendly Version

Interactive Discussion

- Zhang, D. Z. and Iwasaka, Y.: Nitrate and sulfate in individual Asian dust-storm particles in Beijing, China in spring of 1995 and 1996, *Atmos. Environ.*, 33(19), 3213–3223, 1999.
- Zhang, D. Z. and Iwasaka, Y.: Chlorine deposition on dust particles in marine atmosphere, *Geophys. Res. Lett.*, 28(18), 3613–3616, 2001.
- 5 Zhang, D. Z. and Iwasaka, Y.: Size change of Asian dust particles caused by sea salt interaction: Measurements in southwestern Japan, *Geophys. Res. Lett.*, 31(15), doi:10.1029/2004GL020087, 2004.
- Zhang, D. Z., Iwasaka, Y., Shi, G. Y., Zang, J. Y., Matsuki, A., and Trochkin, D.: Mixture state and size of Asian dust particles collected at southwestern Japan in spring 2000, *J. Geophys. Res.*, 108(D24), doi:10.1029/2003JD003869, 2003.
- 10 Zhang, D. Z., Shi, G. Y., Iwasaka, Y., and Hu, M.: Mixture of sulfate and nitrate in coastal atmospheric aerosols: individual particle studies in Qingdao (36 degrees 04' N, 120 degrees 21' E), China, *Atmos. Environ.*, 34(17), 2669–2679, 2000.
- Zhang, J., Chameides, W. L., Weber, R., Cass, G., Orsini, D., Edgerton, E., Jongejan, P., and Slanina, J.: An evaluation of the thermodynamic equilibrium assumption for fine particulate composition: Nitrate and ammonium during the 1999 Atlanta Supersite Experiment, *J. Geophys. Res.*, 108(D7), doi:10.1029/2001JD001592, 2002.
- 15 Zhang, Y. and Carmichael, G. R.: The role of mineral aerosol in tropospheric chemistry in East Asia – A model study, *J. Appl. Meteorol.*, 38(3), 353–366, 1999.
- Zhu, X., Prospero, J. M., Millero, F. J., Savoie, D. L., and Brass, G. W.: The solubility of ferric ion in marine mineral aerosol solutions at ambient relative humidities, *Mar. Chem.*, 38(1–2), 91–107, 1992.
- 20 Zhu, X. R., Prospero, J. M., and Millero, F. J.: Diel variability of soluble Fe(II) and soluble total Fe in North African dust in the trade winds at Barbados, *J. Geophys. Res.*, 102(D17), 21 297–21 305, 1997.
- 25 Zhuang, H., Chan, C. K., Fang, M., and Wexler, A. S.: Size distributions of particulate sulfate, nitrate, and ammonium at a coastal site in Hong Kong, *Atmos. Environ.*, 33(6), 843–853, 1999.
- Zuo, Y. G. and Zhan, J.: Effects of oxalate on Fe-catalyzed photooxidation of dissolved sulfur dioxide in atmospheric water, *Atmos. Environ.*, 39(1), 27–37, 2005.
- 30

**Table 1.** Ion assignments for commonly observed peaks from mineral dust particles and secondary species.

Mass-to-charge ratio	Most probable ion assignment
	Mineral dust
+7	$\text{Li}^+$
+23	$\text{Na}^+$
+27 > 5000	$\text{Al}^+$
+28	$\text{Mg}^+$
+39	$^{39}\text{K}^+$
+40	$\text{Ca}^+$
+41	$^{41}\text{K}^+$ or $[\text{Na}(\text{H}_2\text{O})]^+$
+48	$\text{Ti}^+$
+54	$^{54}\text{Fe}^+$
+56	$^{56}\text{Fe}^+$ or $[\text{CaO}]^+$
+64	$[\text{TiO}]^+$
+96	$[\text{Ca}_2\text{O}]^+$
+112	$[\text{Ca}(\text{O})_2]^+$
+113	$[\text{Ca}(\text{O})_2\text{H}]^+$
-16	$\text{O}^-$
-17	$[\text{OH}]^-$
-26	$[\text{CN}]^-$
-42	$[\text{CNO}]^-$
-43	$[\text{AlO}]^-$
-60	$[\text{AlO}(\text{OH})]^-$ or $[\text{SiO}_2]^-$
-63	$[\text{PO}_2]^-$
-76	$[\text{AlO}_2(\text{OH})]^-$ or $[\text{H}^{28}\text{SiO}_3]^-$
-77	$[\text{H}^{29}\text{SiO}_3]^-$ or $[\text{H}^{28}\text{SiO}_3]^-$
-79	$[\text{PO}_3]^-$
-88	$[\text{SiO}_2]^-$ or $[\text{FeO}]^-$

Title Page

Abstract

Introduction

Conclusions

References

Tables

Figures

◀

▶

◀

▶

Back

Close

Full Screen / Esc

Printer-friendly Version

Interactive Discussion

## Processing of Asian dust

R. C. Sullivan et al.

**Table 1.** Continued.

Mass-to-charge ratio	Most probable ion assignment
	Secondary species
+18 *	$[\text{NH}_4]^+$
+30	$\text{NO}^+$
-32	$\text{S}^-$
-35 *	$^{35}\text{Cl}^-$
-37	$^{37}\text{Cl}^-$
-46	$[\text{NO}_2]^-$
-48	$[\text{SO}]^-$
-62 *	$[\text{NO}_3]^-$
-64	$[\text{SO}_2]^-$
-80	$[\text{SO}_3]^-$
-97 *	$[\text{HSO}_4]^-$

\* indicates the principle ions used to measure ammonium, chloride, nitrate, or sulphate, respectively, in mineral dust particles

Title Page

Abstract

Introduction

Conclusions

References

Tables

Figures

◀

▶

◀

▶

Back

Close

Full Screen / Esc

Printer-friendly Version

Interactive Discussion

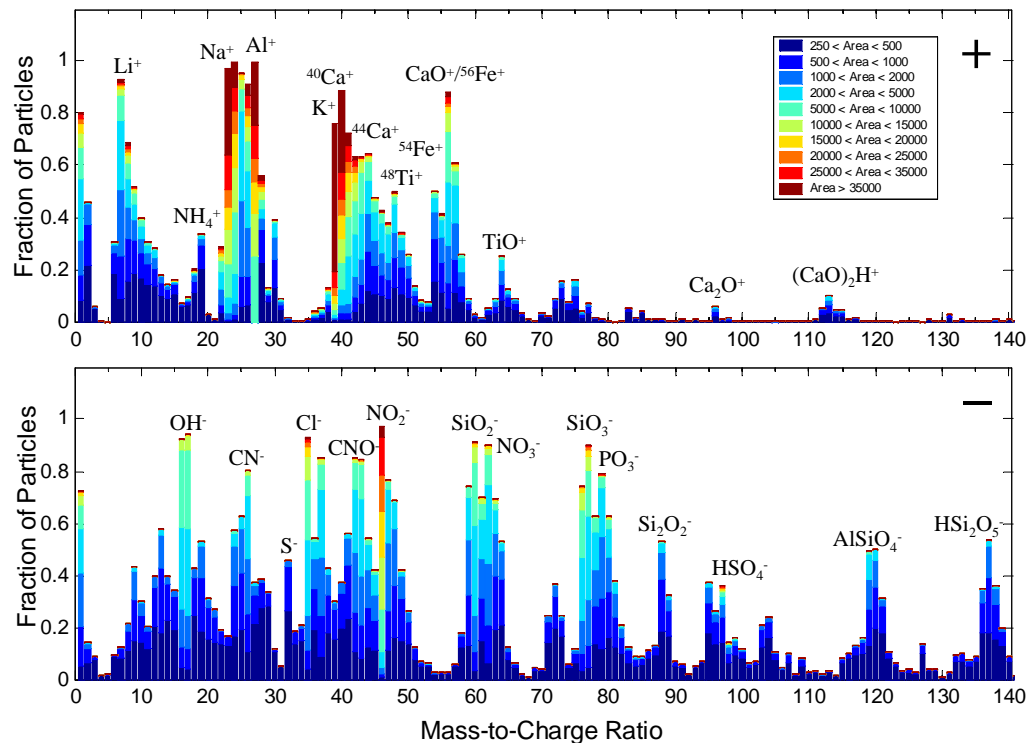


**Fig. 1.** Atmospherically processed mineral dust. Average digital mass spectrum of all 3634 filtered mineral dust particles detected during the dust front's passage over the RHB from DOY 101–101.3. Peaks are assigned to the most likely ions for dust particles (Table 1).

[Title Page](#)
[Abstract](#)
[Introduction](#)
[Conclusions](#)
[References](#)
[Tables](#)
[Figures](#)
[◀](#)
[▶](#)
[◀](#)
[▶](#)
[Back](#)
[Close](#)
[Full Screen / Esc](#)
[Printer-friendly Version](#)
[Interactive Discussion](#)

Processing of Asian  
dust

R. C. Sullivan et al.

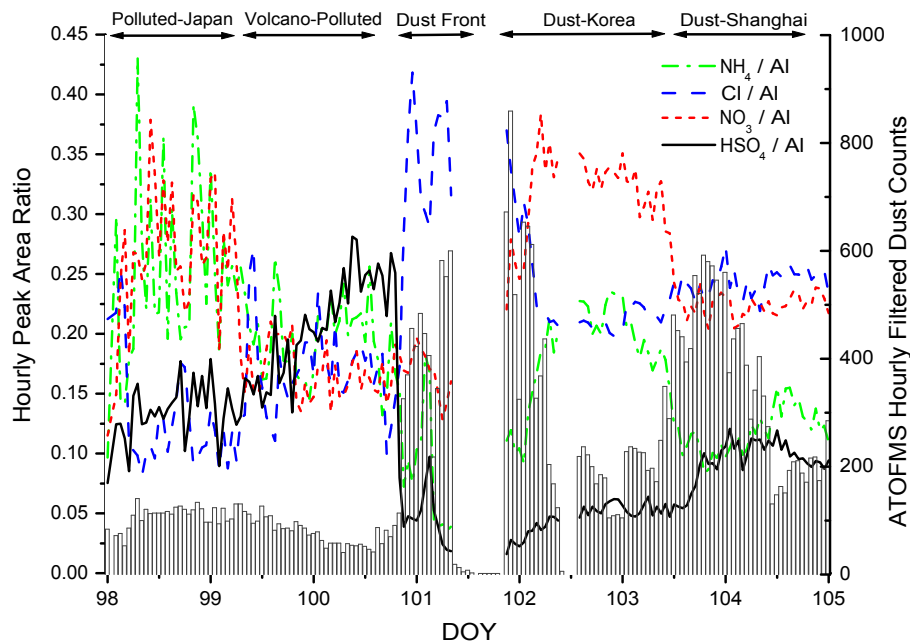


**Fig. 2.** Temporal evolution of secondary species in Asian mineral dust sampled aboard the R/V Ronald Brown. Hourly averaged single-particle peak area ratios (lines) from all filtered dust particles for four major secondary species:  $\text{NH}_4^+$  ( $m/z=18/m/z=27$ ),  $\text{Cl}^-$  ( $m/z=-35/m/z=27$ ),  $\text{NO}_3^-$  ( $m/z=-62/m/z=27$ ), and  $\text{HSO}_4^-$  ( $m/z=-97/m/z=27$ ). Total hourly ATOFMS dust particle counts (bars) are also displayed. Time periods corresponding to different air mass source regions as described by Bates et al. (2004) are indicated. All times are in UTC.

[Title Page](#)[Abstract](#)[Introduction](#)[Conclusions](#)[References](#)[Tables](#)[Figures](#)[◀](#)[▶](#)[◀](#)[▶](#)[Back](#)[Close](#)[Full Screen / Esc](#)[Printer-friendly Version](#)[Interactive Discussion](#)

EGU

## Processing of Asian dust

R. C. Sullivan et al.

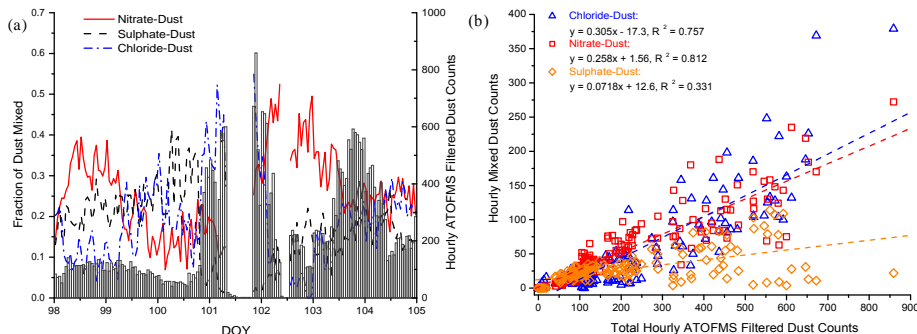


**Fig. 3.** Percentage of dust particles mixed with secondary acids. **(a)** Average hourly fraction (lines) of filtered dust particles defined as mixed with the indicated secondary acid product using the peak area > 5000 criteria for  $^{35}\text{Cl}^-$ ,  $^{62}[\text{NO}_3]^-$  or  $^{97}[\text{HSO}_4]^-$ . The total filtered dust particle hourly counts are also displayed for reference (bars). **(b)** Scatter plot of the hourly counts of dust mixed with one of the three secondary acid products versus the total hourly ATOFMS dust counts, and their least-squares fits.

Title Page

Abstract

Introduction

Conclusions

References

Tables

Figures

◀

▶

◀

▶

Back

Close

Full Screen / Esc

Printer-friendly Version

Interactive Discussion

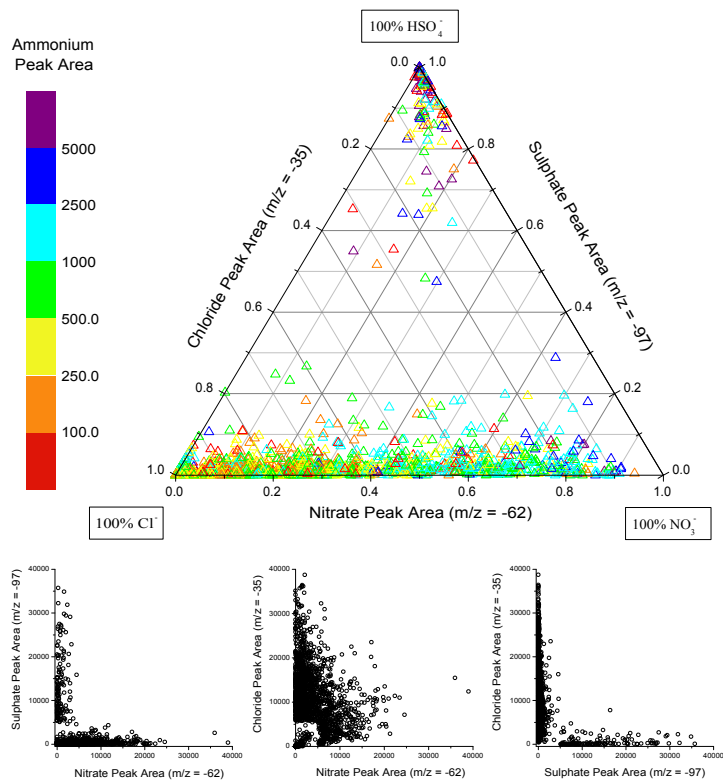


**Fig. 4a.** The ternary plot (top) shows the relative distribution of peak areas for secondary chloride, nitrate, and sulphate in filtered mineral dust particles defined as “mixed” with either of the three acid products and detected during the Dust Front time period (DOY 101–101.3). Each point is produced from a single dust particles mass spectrum, 1768 in total are plotted. The symbol colour corresponds to the absolute peak area of ammonium for each dust particle. The scatter plots (below) for pairs of secondary acid products are taken from the same data set and show the same trends as the ternary plot but on an absolute peak area scale.

Title Page

Abstract

Introduction

Conclusions

References

Tables

Figures

◀

▶

◀

▶

Back

Close

Full Screen / Esc

Printer-friendly Version

Interactive Discussion

Processing of Asian  
dust

R. C. Sullivan et al.

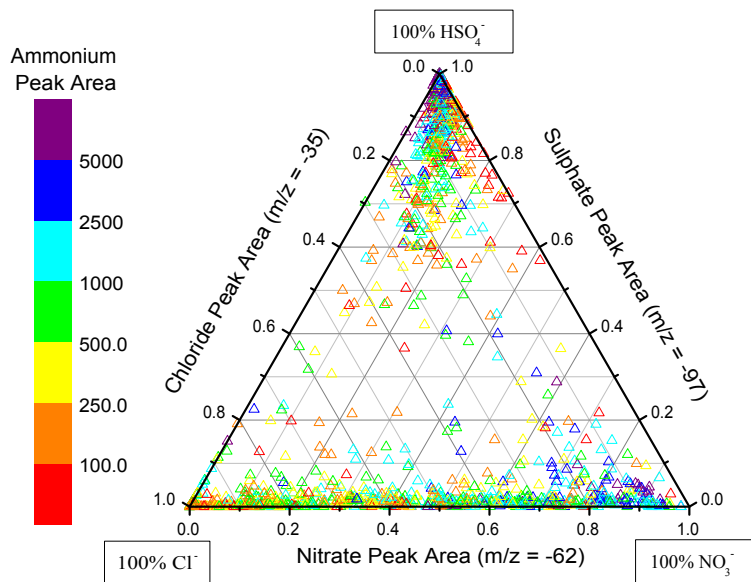


**Fig. 4b.** As for (a) above but for dust particles detected during the Polluted Volcano time period (DOY 99.3–100.5). Each point is produced from a single dust particles mass spectrum, 1361 in total are plotted.

[Title Page](#)[Abstract](#)[Introduction](#)[Conclusions](#)[References](#)[Tables](#)[Figures](#)[◀](#)[▶](#)[◀](#)[▶](#)[Back](#)[Close](#)[Full Screen / Esc](#)[Printer-friendly Version](#)[Interactive Discussion](#)

EGU

Processing of Asian  
dust

R. C. Sullivan et al.

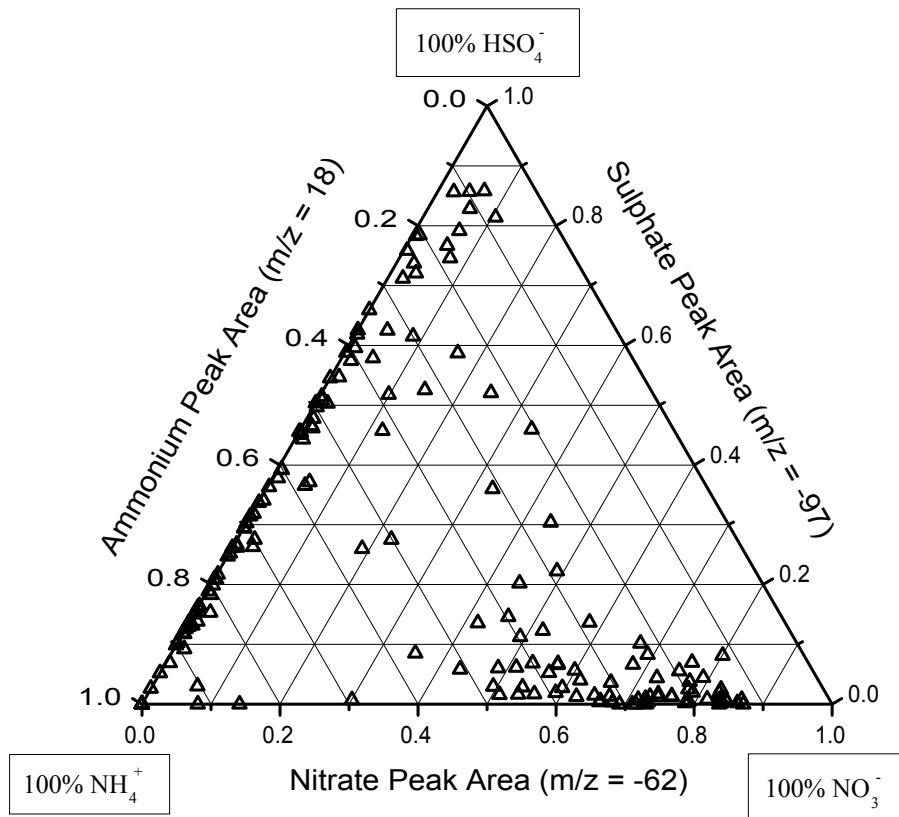


**Fig. 5.** Relative distribution of absolute peak areas for nitrate, sulphate, and ammonium in nitrate-dust or sulphate-dust satisfying a peak area for  $m/z$  18 > 1000, detected during the Polluted Volcano time period. 364 dust particles are displayed.

[Title Page](#)[Abstract](#)[Introduction](#)[Conclusions](#)[References](#)[Tables](#)[Figures](#)[◀](#)[▶](#)[◀](#)[▶](#)[Back](#)[Close](#)[Full Screen / Esc](#)[Printer-friendly Version](#)[Interactive Discussion](#)

EGU

## Processing of Asian dust

R. C. Sullivan et al.

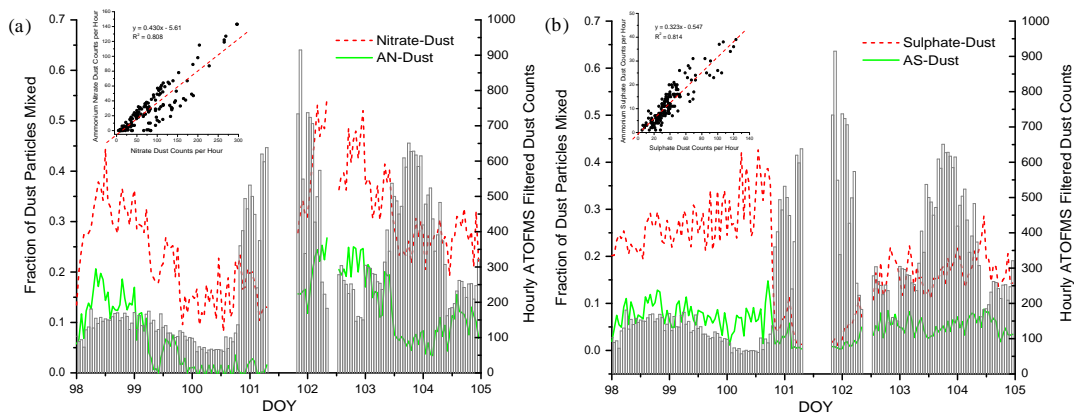


**Fig. 6.** The fractions of filtered dust particles (lines) classified as mixed with **(a)** nitrate or ammonium nitrate (AN); **(b)** sulphate or ammonium sulphate (AS); and the total hourly filtered dust counts (bars). Scatter plots (insets) show the correlation between hourly counts of nitrate/sulphate dust and ammonium nitrate/sulphate dust. The slope of the linear fit indicates the average hourly fraction of nitrate- or sulphate-dust that was also mixed with ammonium.

Title Page

Abstract

Introduction

Conclusions

References

Tables

Figures

◀

▶

◀

▶

Back

Close

Full Screen / Esc

Printer-friendly Version

Interactive Discussion

EGU

## Processing of Asian dust

R. C. Sullivan et al.

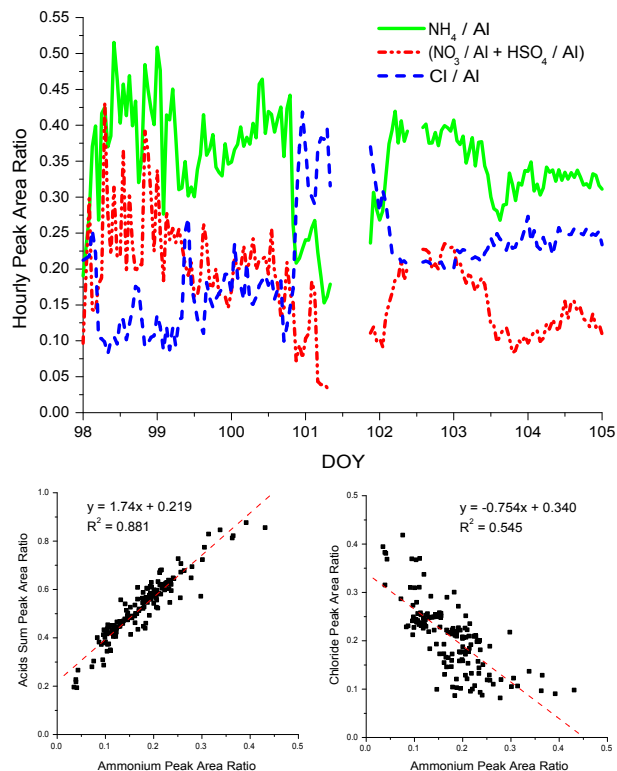


**Fig. 7.** Correlation between ammonium and acids in dust. Top: Hourly peak area ratios for ammonium (18/27), chloride (–35/27) and the sum of nitrate (–62/27) plus sulphate (–97/27) for all filtered dust particles from DOY 98–105. Bottom: Scatter plots of the correlation between ammonium and sum of chloride + nitrate + sulphate hourly peak area ratios for this time period (left), the hourly peak area ratios of chloride and ammonium (right), and the corresponding least-squares linear fits.

[Title Page](#)[Abstract](#)[Introduction](#)[Conclusions](#)[References](#)[Tables](#)[Figures](#)[◀](#)[▶](#)[◀](#)[▶](#)[Back](#)[Close](#)[Full Screen / Esc](#)[Printer-friendly Version](#)[Interactive Discussion](#)

Processing of Asian  
dust

R. C. Sullivan et al.

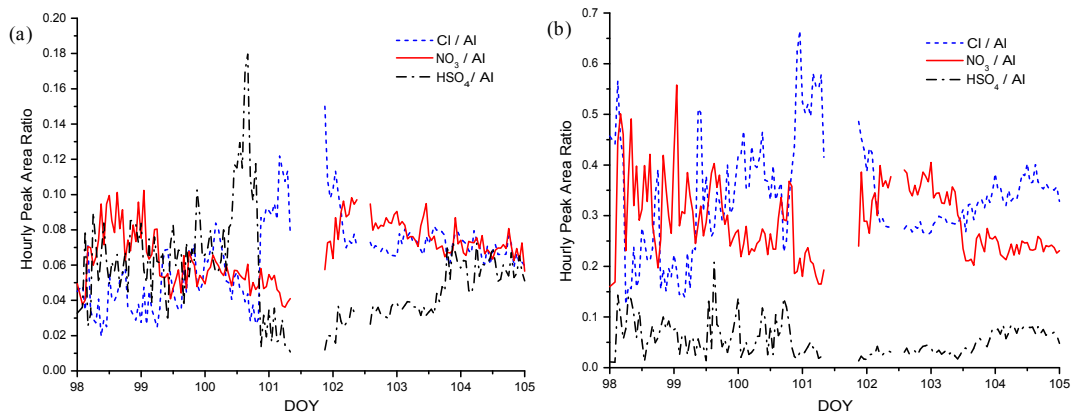


**Fig. 8.** Hourly peak area ratios of the three major secondary acid reaction products: chloride, nitrate and sulphate, for filtered dust particles high in Al (a) or in Ca (b).

[Title Page](#)[Abstract](#)[Introduction](#)[Conclusions](#)[References](#)[Tables](#)[Figures](#)[◀](#)[▶](#)[◀](#)[▶](#)[Back](#)[Close](#)[Full Screen / Esc](#)[Printer-friendly Version](#)[Interactive Discussion](#)

EGU

## Processing of Asian dust

R. C. Sullivan et al.

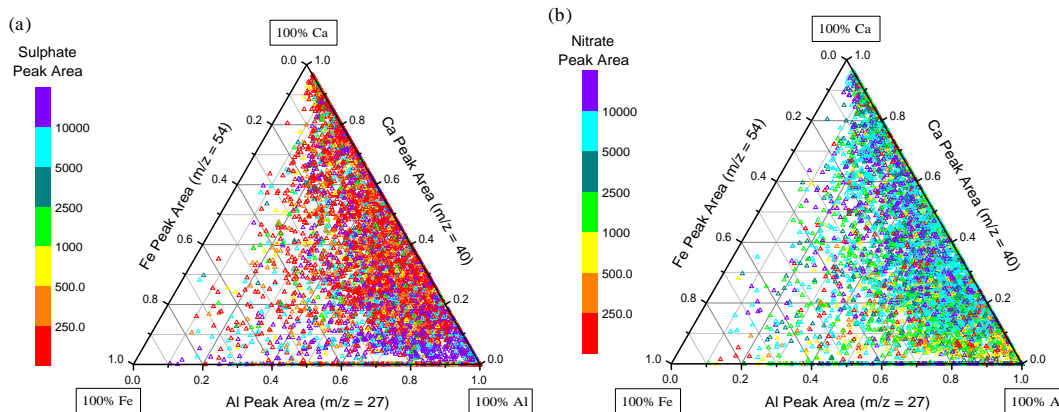


**Fig. 9.** Relative distribution of peak areas for three major mineral components, Fe, Ca, and Al, for filtered dust particles significantly mixed with secondary acids and detected during the Dust & Shanghai time period. The same 5812 dust particles are displayed in both figures with the symbol colour corresponding to the sulphate absolute peak area (a), or the nitrate absolute peak area (b).

[Title Page](#)[Abstract](#)[Introduction](#)[Conclusions](#)[References](#)[Tables](#)[Figures](#)[◀](#)[▶](#)[◀](#)[▶](#)[Back](#)[Close](#)[Full Screen / Esc](#)[Printer-friendly Version](#)[Interactive Discussion](#)

EGU

## Processing of Asian dust

R. C. Sullivan et al.

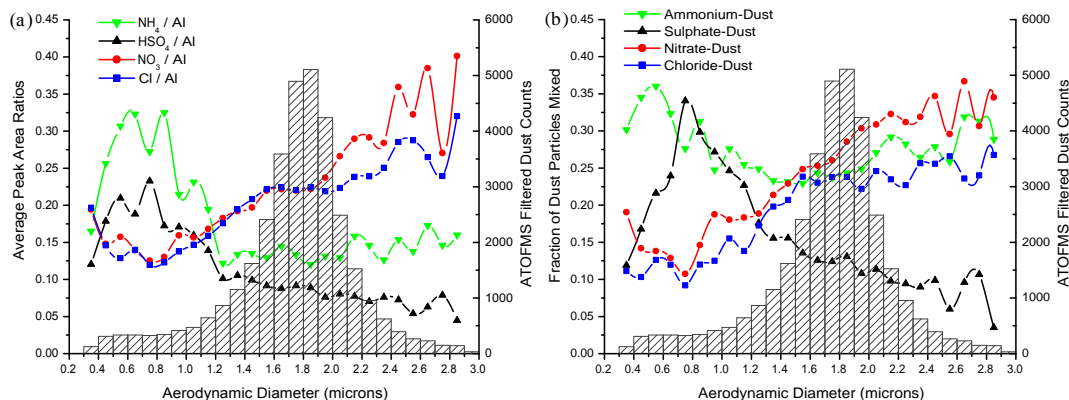


**Fig. 10.** Size distributions of secondary species in mineral dust particles. **(a)** Average peak areas ratios (lines) for four major secondary species from all filtered dust particles detected from DOY 98–105. **(b)** Fraction of filtered dust particles (lines) classified as mixed with one of the four major secondary species. The size distribution of the set of particles used to generate both figures is also displayed (columns) and reflects the inlet efficiency of the ATOFMS, and not the actual size distribution of the aerosol population.

[Title Page](#)[Abstract](#)[Introduction](#)[Conclusions](#)[References](#)[Tables](#)[Figures](#)[◀](#)[▶](#)[◀](#)[▶](#)[Back](#)[Close](#)[Full Screen / Esc](#)[Printer-friendly Version](#)[Interactive Discussion](#)

EGU